

Federated Learning with Sparsified Model Perturbation: Improving Accuracy under Client-Level Differential Privacy

Rui Hu, *Student Member, IEEE*, Yanmin Gong, *Senior Member, IEEE* and Yuanxiong Guo, *Senior Member, IEEE*

Abstract—Federated learning (FL) that enables distributed clients to collaboratively learn a shared statistical model while keeping their training data locally has received great attention recently and can improve privacy and communication efficiency in comparison with traditional centralized machine learning paradigm. However, sensitive information about the training data can still be inferred from model updates shared in FL. Differential privacy (DP) is the state-of-the-art technique to defend against those attacks. The key challenge to achieve DP in FL lies in the adverse impact of DP noise on model accuracy, particularly for deep learning models with large numbers of model parameters. This paper develops a novel differentially-private FL scheme named Fed-SMP that provides client-level DP guarantee while maintaining high model accuracy. To mitigate the impact of privacy protection on model accuracy, Fed-SMP leverages a new technique called Sparsified Model Perturbation (SMP), where local models are sparsified first before being perturbed with additive Gaussian noise. Two sparsification strategies are considered in Fed-SMP: random sparsification and top- k sparsification. We also apply Rényi differential privacy to providing a tight analysis for the end-to-end DP guarantee of Fed-SMP and prove the convergence of Fed-SMP with general loss functions. Extensive experiments on real-world datasets are conducted to demonstrate the effectiveness of Fed-SMP in largely improving model accuracy with the same level of DP guarantee and saving communication cost simultaneously.

I. INTRODUCTION

The proliferation of edge devices such as smartphones and Internet-of-things (IoT) devices, each equipped with rich sensing, computation, and storage resources, leads to tremendous data being generated on a daily basis at the network edge. These data can be analyzed to build machine learning models that enable a wide range of intelligent services such as personal fitness tracking [1], traffic monitoring [2], and smart home security [3]. Traditional machine learning paradigm requires transferring all the raw data to the cloud before training a model, leading to high communication cost and severe privacy risk.

As an alternative machine learning paradigm, *Federated Learning (FL)* has attracted significant attention recently due to its benefits in communication efficiency and privacy [4]. In

FL, multiple clients collaboratively learn a shared statistical model under the orchestration of the cloud without sharing their local data [5]. Although only model updates are shared instead of raw data by each client in FL, it is not sufficient to ensure privacy as the sensitive training data can still be inferred from the shared local model updates by advanced inference attacks. For instance, given an input sample and a target model, the membership inference attack [6] can train an attack model to determine whether the sample was used for training the target model or not. Also, given a target model and class, the model inversion attack [7] can recover the typical sample representations of the target class using an inversion model learned from the correlation between the inputs and outputs of the target model.

As a cryptography-inspired rigorous definition of privacy, differential privacy (DP) has become the de-facto standard for achieving data privacy and can give strong privacy guarantee against an adversary with arbitrary auxiliary information [8]. For privacy protection in FL, client-level DP is often more relevant than record-level DP: client-level DP guarantee protects the participation of a client, while record-level DP guarantee protects only a single data sample of a client [9], [10]. While DP can be straightforwardly achieved using Gaussian or Laplacian mechanism [8], achieving client-level DP in the FL setting faces several major challenges in maintaining high model accuracy. First of all, FL is an iterative learning process where model updates are exchanged in multiple rounds, leading to more privacy leakage compared to the one-shot inference. Secondly, the intensity of added DP noise is linearly proportional to the model size, which can be very large (e.g., millions of model parameters) for modern deep neural networks (DNNs), and will severely degrade the accuracy of the trained model. Thirdly, it is more challenging to achieve client-level DP than record-level DP because the entire dataset of a client rather than a single data sample of that client needs to be protected. Existing studies [11]–[13] on FL with client-level DP guarantee suffer from significant accuracy degradation due to the inherent challenge of large additive random noise required to achieve a certain level of client-level DP for DNNs.

In this paper, we propose a new differentially-private FL scheme called *Fed-SMP*, which guarantees client-level DP while preserving model accuracy and saving communication

R. Hu and Y. Gong are with the Department of Electrical and Computer Engineering, University of Texas at San Antonio, San Antonio, TX, 78249 USA (e-mail: {rui.hu, yanmin.gong}@utsa.edu).

Y. Guo is with the Department of Information Systems and Cyber Security, University of Texas at San Antonio, San Antonio, TX, 78249 USA (e-mail: yuanxiong.guo@utsa.edu).

cost simultaneously. Fed-SMP utilizes *Sparsified Model Perturbation (SMP)* to improve the privacy-accuracy tradeoff of DP in FL. Specifically, SMP first sparsifies the local model update of a client at each round by selecting only a subset of coordinates to keep and then adds Gaussian noise to perturb the values at those selected coordinates. As we will show later in this paper, by using SMP in FL, the sparsification will have an amplification effect on the privacy guarantee offered by the added Gaussian noise, leading to a better privacy-accuracy tradeoff. Meanwhile, it can reduce the communication cost by compressing the shared model updates at each round. In summary, the main contributions of this paper are summarized as follows.

- We propose a new differentially-private FL scheme called Fed-SMP to improve the privacy-utility tradeoff of FL with client-level DP. By using sparsification as a tool for amplifying privacy and reducing communication cost at the same time, the proposed method can achieve both goals of privacy protection and communication efficiency at little cost on model accuracy. Fed-SMP only makes lightweight modifications to FedAvg [5], the most common learning method for FL, which enables easy integration into existing packages.
- We design two algorithms of Fed-SMP based on different sparsification operators: Fed-SMP with random sparsification and Fed-SMP with top- k sparsification. The resulting algorithms require less amount of added random noise to achieve the same level of DP and are compatible with secure aggregation, which is a key privacy-enhancing technique to achieve client-level DP in practical FL systems.
- We theoretically analyze the impact of model sparsification on the convergence of Fed-SMP under (ϵ, δ) -DP guarantee and show that the optimal compression level needs to balance the increased compression error and reduced privacy error due to sparsification.
- We empirically evaluate the performances of the proposed schemes on Fashion-MNIST and SVHN datasets and compare the results with those of the state-of-art baselines. Experimental results demonstrate that Fed-SMP can achieve higher model accuracy than baseline approaches under the same level of DP while saving communication cost.

The rest of the paper is organized as follows. Preliminaries on DP and secure aggregation protocol used in this paper are described in Section II. Section III introduces the problem formulation and presents the proposed Fed-SMP scheme. The privacy and convergence properties of Fed-SMP with random and top- k sparsification strategies are rigorously analyzed in Section V. Section VI shows the experimental results. Finally, Section VII reviews the related work, and Section VIII concludes the paper.

II. PRELIMINARIES

A. Differential Privacy in Machine Learning

DP has been proposed as a rigorous privacy notion for measuring privacy risk. The classic notion of DP, (ϵ, δ) -DP, is defined as follows:

Definition 1 ((ϵ, δ) -DP [8]). *Given privacy parameters $\epsilon > 0$ and $0 \leq \delta < 1$, a randomized mechanism \mathcal{M} satisfies (ϵ, δ) -DP if for any two adjacent datasets D, D' and any subset of outputs $O \subseteq \text{range}(\mathcal{M})$,*

$$\Pr[\mathcal{M}(D) \in O] \leq e^\epsilon \Pr[\mathcal{M}(D') \in O] + \delta. \quad (1)$$

When $\delta = 0$, we have ϵ -DP, or Pure DP.

To better account the privacy loss over multiple iterations in differentially private learning algorithms, Rényi differential privacy (RDP) has been proposed as follows:

Definition 2 ((α, ρ) -RDP [14]). *Given a real number $\alpha > 1$ and privacy parameter $\rho \geq 0$, a randomized mechanism \mathcal{M} satisfies (α, ρ) -RDP if for any two adjacent datasets D, D' , the Rényi α -divergence between $\mathcal{M}(D)$ and $\mathcal{M}(D')$ satisfies*

$$D_\alpha[\mathcal{M}(D) \parallel \mathcal{M}(D')] := \frac{1}{\alpha - 1} \log \mathbb{E} \left[\left(\frac{\mathcal{M}(D)}{\mathcal{M}(D')} \right)^\alpha \right] \leq \rho(\alpha).$$

RDP is a relaxed version of pure DP with a tighter composition bound. Thus it is more suitable to analyze the end-to-end privacy loss of iterative algorithms. We can convert RDP to (ϵ, δ) -DP for any $\delta > 0$ using the following lemma:

Lemma 1 (From RDP to (ϵ, δ) -DP [15]). *If the randomized mechanism \mathcal{M} satisfies $(\alpha, \rho(\alpha))$ -RDP, then it also satisfies $(\rho(\alpha) + \frac{\log(1/\delta)}{\alpha - 1}, \delta)$ -DP.*

In the following, we provide some useful definitions and lemmas about DP and RDP that will be used to derive our main results in the rest of the paper.

Definition 3 (ℓ_2 -sensitivity [8]). *Let $h : \mathcal{D} \rightarrow \mathbb{R}^d$ be a query function over a dataset. The ℓ_2 -sensitivity of h is defined as $\psi(h) := \sup_{D, D' \in \mathcal{D}, D \sim D'} \|h(D) - h(D')\|_2$ where $D \sim D'$ denotes that D and D' are two adjacent datasets.*

Lemma 2 (Gaussian Mechanism [14]). *Let $h : \mathcal{D} \rightarrow \mathbb{R}^d$ be a query function with ℓ_2 -sensitivity $\psi(h)$. The Gaussian mechanism $\mathcal{M} = h(D) + \mathcal{N}(0, \sigma^2 \psi(h)^2 \cdot \mathbf{I}_d)$ satisfies $(\alpha, \alpha/2\sigma^2)$ -RDP.*

Lemma 3 (RDP for Subsampling Mechanism [15], [16]). *For a Gaussian mechanism \mathcal{M} and any m -datapoints dataset D , define $\mathcal{M} \circ \text{SUBSAMPLE}$ as 1) subsample without replacement B datapoints from the dataset (denote $q = B/m$ as the sampling ratio); and 2) apply \mathcal{M} on the subsampled dataset as input. Then if \mathcal{M} satisfies $(\alpha, \rho(\alpha))$ -RDP with respect to the subsampled dataset for all integers $\alpha \geq 2$, then the new*

randomized mechanism $\mathcal{M} \circ \text{SUBSAMPLE}$ satisfies $(\alpha, \rho'(\alpha))$ -RDP with respect to D , where

$$\rho'(\alpha) \leq \frac{1}{\alpha-1} \log \left(1 + q^2 \binom{\alpha}{2} \min\{4(e^{\rho(2)} - 1), 2e^{\rho(2)}\} + \sum_{j=3}^{\alpha} q^j \binom{\alpha}{j} 2e^{(j-1)\rho(j)} \right).$$

If $\sigma^2 \geq 0.7$ and $\alpha \leq (2/3)\sigma^2\psi^2(h) \log(1/q\alpha(1+\sigma^2)) + 1$, $\mathcal{M} \circ \text{SUBSAMPLE}$ satisfies $(\alpha, 3.5q^2\alpha/\sigma^2)$ -RDP.

Lemma 4 (RDP Composition [14]). *For randomized mechanisms \mathcal{M}_1 and \mathcal{M}_2 applied on dataset D , if \mathcal{M}_1 satisfies (α, ρ_1) -RDP and \mathcal{M}_2 satisfies (α, ρ_2) -RDP, then their composition $\mathcal{M}_1 \circ \mathcal{M}_2$ satisfies $(\alpha, \rho_1 + \rho_2)$ -RDP.*

B. Secure Aggregation in FL

As a key privacy-enhancing technique in FL, secure aggregation is a lightweight instance of cryptographic secure multi-party computation that prevents the server from inspecting individual model updates of clients in FL [17]. It enables the server to learn just an aggregate function of the clients' local model updates, typically the sum, and nothing else. In the typical setting of FL with a single server, secure aggregation is achieved by adding random mask vectors sampled over a finite group on local model updates before sending them out [18]. Specifically, clients generate randomly sampled zero-sum mask vectors locally by working in the space of integers modulo m and sampling the elements of the mask uniformly from \mathbb{Z}_m . Secure aggregation in FL ensures that the masked local model update is indistinguishable from random values, revealing no further information to potential adversaries. However, when the server computes the modular sum of all the masked updates, the masks cancel out and the server obtains the exact sum of local model updates. As with the existing works in FL [19]–[21], we ignore the finite precision and modular summation arithmetic associated with secure aggregation in this paper, noting that one can follow the strategy in [22] to transform the real valued vectors into integers for minimizing the approximation error of recovering the sum.

C. Record-level and Client-level DP in FL

The DP definitions in Section II-A apply to a range of different granularity, depending on how the adjacent datasets are defined. In this paper, we define the adjacent datasets by adding or removing the entire local data of a client, and aim to protect whether one client participates into training or not in FL. This is known as *client-level DP* [11]. In comparison, the commonly used privacy notion in standard non-federated learning DP is *record-level DP* [10], where the adjacent datasets are defined by adding or removing a single training example of a client, and only the privacy of one training example is protected. Therefore, client-level DP is stronger than record-level DP and has been shown to be more relevant to practical FL applications with a large number of clients [11].

III. SYSTEM MODELING AND PROBLEM FORMULATION

In this section, we first present the problem formulation of FL and attack model, and then describe the classic method to solve the problem as well as its privacy-preserving variant.

A. Problem Formulation

A typical FL system consists of n clients (e.g., smartphones or IoT devices) and a central server (e.g., the cloud), as shown in Figure 1. Each client $i \in [n]$ has a local dataset of m samples, and those clients collaboratively train a global model $\theta \in \mathbb{R}^d$ based on their collective datasets under the orchestration of the central server. The goal of FL is to solve the following optimization problem:

$$\min_{\theta \in \mathbb{R}^d} f(\theta) := \frac{1}{n} \sum_{i \in [n]} f_i(\theta), \quad (2)$$

where $f_i(\theta) = (1/m) \sum_{z \in D_i} l(\theta; z)$ is the local objective function of client i . Here, D_i represents the dataset of client i , z represents a datapoint sampled from D_i , and $l(\theta; z)$ denotes the loss of model θ on datapoint z . For $i \neq j$, the data distributions of D_i and D_j may be different.

B. Attack Model

The adversary can be the “honest-but-curious” server or clients in the system. The adversary will honestly follow the designed training protocol but is curious about a target client's private data and wants to infer it from the shared messages. Furthermore, some clients can collude with the server or each other to infer private information about a specific victim client. Besides, the adversary could also be the passive outside attacker. These attackers can eavesdrop all the shared messages during the execution of the training but will not actively inject false messages into or interrupt message transmissions.

C. Achieving Client-level DP in FL

As the classic and most widely-used algorithm in the FL setting, Federated Averaging (FedAvg) [5] solves (2) by running multiple iterations of stochastic gradient descent (SGD) in parallel on a subset of clients and then averaging the resulting local model updates at a central server periodically. Compared with distributed SGD, FedAvg is shown to achieve the same model accuracy with fewer communication rounds. Specifically, FedAvg involves T communication rounds, and each round can be divided into four stages as shown in Figure 1. First, at the beginning of round $t \in \{0, \dots, T-1\}$, the server randomly selects a subset \mathcal{W}^t of r clients and sends them the latest global model θ^t to perform local computations. Second, each client $i \in \mathcal{W}^t$ runs τ iterations of SGD on its local dataset to update its local model. Let $\theta_i^{t,s}$ denote client i 's model after the s -th local iteration at the t -th communication round where $s \in [0, \tau-1]$. By model initialization, we have $\theta_i^{t,0} = \theta^t$. Then the update rule at client i is represented as

$$\theta_i^{t,s+1} = \theta_i^{t,s} - \eta_l \mathbf{g}_i^{t,s}, \forall s = 0, \dots, \tau-1, \quad (3)$$

where η_l is the local learning rate and $\mathbf{g}_i^{t,s} := (1/B) \sum_{z \in \mathcal{C}_i^{t,s}} \nabla l(\theta_i^{t,s}, z)$ represents the stochastic gradient

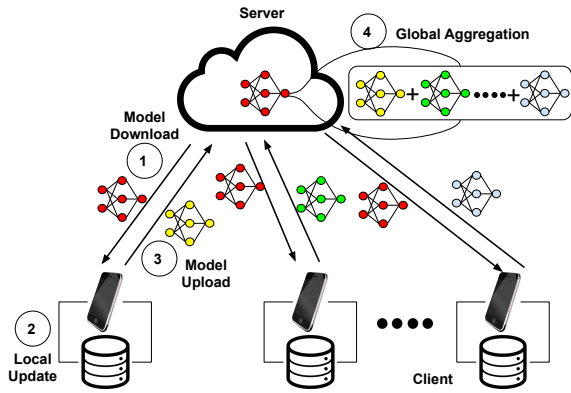


Figure 1: An exemplary FL system.

over a mini-batch $\xi_i^{t,s}$ of B datapoints sampled from D_i . Third, the client i uploads its model update $\Delta_i^t := \theta^t - \theta_i^{t,\tau}$ to the server. Fourth, after receiving all the local model updates, the server updates the global model by

$$\theta^{t+1} = \theta^t - \frac{1}{r} \sum_{i \in \mathcal{W}^t} \Delta_i^t. \quad (4)$$

The same procedure repeats at the next round $t+1$ thereafter until satisfying certain convergence criteria.

In FedAvg, clients need to repeatedly upload the local model updates of large dimension d (e.g., millions of model parameters for DNNs) to the server and download the newly-updated global model from the server for many times in order to learn an accurate global model. Since the bandwidth between the server and clients could be rather limited, especially for uplink transmissions, the overall communication cost could be very high. Furthermore, although FedAvg can avoid the direct information leakage by keeping local dataset on client, the model updates shared at each round can still leak private information about the local dataset as demonstrated in recent advanced attacks such as model inversion attack [7] and membership inference attack [6].

To provide client-level DP in FL without a fully trusted server, prior studies [9], [11] have proposed the following changes to FedAvg at each FL round:

- 1) Clients are randomly selected to perform local computations;
- 2) Each client's model update is clipped to have a bounded ℓ_2 -norm;
- 3) Gaussian noise is added to the clipped model update at each client;
- 4) Noisy local model updates are encrypted following a secure aggregation protocol (e.g., [18]) and then sent to the server for aggregation.

However, the resulting accuracy of the trained model is often low due to the large intensity of added Gaussian noise. Moreover, communication cost has never been considered in those studies. This motivates us to develop a new differentially private FL scheme that can maintain high model accuracy while reducing communication cost.

IV. FED-SMP: FEDERATED LEARNING WITH SPARSIFIED MODEL PERTURBATION

In this section, we develop a new FL scheme called Fed-SMP with the goal of providing client-level DP with high model accuracy while improving communication efficiency at the same time. To ensure easy integration into existing packages/systems, Fed-SMP follows the same overall procedure of FedAvg as depicted in Figure 1 and employs a novel integration of Gaussian mechanism and sparsification in the local update stage. This guarantees that the shared local model update from each client is both sparse and differentially private. The two specific sparsifiers considered in Fed-SMP are defined as follows:

Definition 4 (Random and Top- k Sparsifiers). *For a parameter $1 \leq k \leq d$ and vector $\mathbf{x} \in \mathbb{R}^d$, the random sparsifier $\text{rand}_k : \mathbb{R}^d \times \Omega_k \rightarrow \mathbb{R}^d$ and top- k sparsifier $\text{top}_k : \mathbb{R}^d \rightarrow \mathbb{R}^d$ are defined as*

$$[\text{rand}_k(\mathbf{x}, \omega)]_j := \begin{cases} [\mathbf{x}]_j, & \text{if } j \in \omega \\ 0, & \text{otherwise} \end{cases}, \quad (5)$$

$$[\text{top}_k(\mathbf{x})]_j := \begin{cases} [\mathbf{x}]_{\pi(j)}, & \text{if } j \leq k \\ 0, & \text{otherwise} \end{cases}, \quad (6)$$

where $\Omega_k = \binom{[d]}{k}$ denotes the set of all k -element subsets of $[d]$, ω is chosen uniformly at random, i.e., $\omega \sim_{u.a.r} \Omega_k$, and π is a permutation of $[d]$ such that $|\mathbf{x}_{\pi(j)}| \geq |\mathbf{x}_{\pi(j+1)}|$ for $j \in [1, d-1]$,

In Fed-SMP with both rand_k and top_k sparsifier, only k coordinates of the local model update will be sent out. Generally speaking, rand_k sparsifier may discard coordinates that are actually important, which inevitably degrades model accuracy when k is small. On the other hand, top_k sparsifier keeps the coordinates with the largest magnitude and can achieve higher model accuracy for small k . This seems to indicate that top_k is always the better choice. However, the two sparsifiers have different privacy implications. For rand_k sparsifier, since the set of selected coordinates ω is chosen uniformly at random, the coordinates themselves are not data dependent and thus do not leak any private information of client data. On the other hand, the set of selected coordinates for top_k sparsifier depends on the values of model parameters and hence contains private information of client data and needs to be protected. It is worth noting that although rand_k and top_k sparsifiers are randomized mechanisms, they do not provide any privacy guarantee by themselves in terms of DP and need to be combined with Gaussian mechanism for rigorous DP guarantee.

Using the above sparsifiers for client-level DP in FL has new challenges. As mentioned before, secure aggregation is a key privacy-enhancing technique to achieve client-level DP in practical FL systems. However, the naive application of rand_k or top_k sparsifier to the local model update of each client typically results in a different set of k coordinates for each client, preventing us from only encrypting the k selected

Algorithm 1 Fed-SMP: Federated Learning with Sparsified Model Perturbation

Require: size of selected clients per round r , number of rounds T , local update period τ , learning rate η_l , clipping threshold C , noise multiplier σ , compression parameter k , sparsifier spar (rand_k or top_k), encryption/decryption functions $\text{Enc}(\cdot)$ and $\text{Dec}(\cdot)$ in the secure aggregation protocol.

Server executes:

- 1: Initialize θ^0
- 2: **for** $t = 0$ to $T - 1$ **do**
- 3: Sample a set of r clients uniformly at random without replacement, denoted by $\mathcal{W}^t \subseteq [n]$
- 4: **if** spar is rand_k **then**
- 5: $\mathbf{m}^t \leftarrow \text{SelectRandk}(\theta^t, k)$
- 6: **else if** spar is top_k **then**
- 7: $\mathbf{m}^t \leftarrow \text{SelectTopk}(\theta^t, k)$
- 8: **end if**
- 9: Broadcast θ^t and \mathbf{m}^t to all clients in \mathcal{W}^t
- 10: **for** each clients $i \in \mathcal{W}^t$ **in parallel do**
- 11: $\mathbf{y}_i^t \leftarrow \text{ClientUpdate}(\theta^t, \mathbf{m}^t, \text{spar})$
- 12: **end for**
- 13: $\theta^{t+1} \leftarrow \theta^t - \text{Dec}(\sum_{i \in \mathcal{W}^t} \mathbf{y}_i^t) / r$
- 14: **end for**
- 15: return θ^T

SelectRandk(θ^t, k):

- 16: Select a random set of k coordinates of θ^t and create a corresponding mask vector $\mathbf{m}^t \in \{0, 1\}^d$
- 17: return \mathbf{m}^t

SelectTopk(θ^t, k):

Require: public dataset D_p , update period τ_p

- 18: $\theta_p^0 \leftarrow \theta^t$
- 19: **for** $s = 0$ to $\tau - 1$ **do**
- 20: Compute a mini-batch stochastic gradient \mathbf{g}_p^s over D_p
- 21: $\theta_p^{s+1} \leftarrow \theta_p^s - \eta_l \mathbf{g}_p^s$
- 22: **end for**
- 23: $\Delta_p \leftarrow \theta^t - \theta_p^\tau$
- 24: Select the top k coordinates of $|\Delta_p|$ and create a corresponding mask vector $\mathbf{m}^t \in \{0, 1\}^d$
- 25: return \mathbf{m}^t

ClientUpdate($\theta^t, \mathbf{m}^t, \text{spar}$):

- 26: $\theta_i^{t,0} \leftarrow \theta^t$
- 27: **for** $s = 0$ to $\tau - 1$ **do**
- 28: Compute a mini-batch stochastic gradient $\mathbf{g}_i^{t,s}$
- 29: $\theta_i^{t,s+1} \leftarrow \theta_i^{t,s} - \eta_l \mathbf{g}_i^{t,s}$
- 30: **end for**
- 31: $\Delta_i^t \leftarrow \text{DP-spar}(\theta^t - \theta_i^{t,\tau}, \mathbf{m}^t, \text{spar})$
- 32: return $\text{Enc}(\Delta_i^t)$

DP-spar($\Delta, \mathbf{m}^t, \text{spar}$):

- 33: **if** spar is rand_k **then**
- 34: $\Delta' \leftarrow \frac{d}{k} \times \Delta \odot \mathbf{m}^t$
- 35: **else if** spar is top_k **then**
- 36: $\Delta' \leftarrow \Delta \odot \mathbf{m}^t$
- 37: **end if**
- 38: $\hat{\Delta} \leftarrow \Delta' \times \min(1, C / \|\Delta'\|_2)$
- 39: return $\hat{\Delta} + \mathcal{N}(0, (C^2 \sigma^2 / r) \cdot \mathbf{I}_d) \odot \mathbf{m}^t$

coordinates of each client in the secure aggregation protocol. One can apply secure aggregation to all the d coordinates, but the communication efficiency benefit of sparsification will get lost. In the following, we design new rand_k and top_k sparsifiers in Fed-SMP that are compatible with secure aggregation. Specifically, we let the selected clients keep the same set of k active coordinates at each round; therefore, those clients can transmit the sparsified model update directly using the secure aggregation protocol and save communication cost.

The pseudo-code for the proposed Fed-SMP is provided in Algorithm 1. At the beginning of round t , the server randomly selects a set \mathcal{W}^t of r clients and broadcasts to them the current global model θ^t and mask vector $\mathbf{m}^t \in \{0, 1\}^d$ (lines 3-9). The j -th coordinate of mask vector \mathbf{m}^t equals to 1 if that coordinate is selected by the sparsifier at round t and 0 otherwise. In Fed-SMP with rand_k sparsifier, the k coordinates are selected randomly from $[d]$ by the server (i.e., the procedure **SelectRandk**(\cdot)). In Fed-SMP with top_k sparsifier, we let the server choose a set of top k coordinates for all clients using a public dataset D_p at each round, avoiding privacy leakage from the selected coordinates. The public dataset D_p is assumed to have a similar distribution to the overall data distribution of

all clients' collective dataset. The assumption of such a public dataset is common in FL literature [23], [24]. Specifically, at round t , the server first performs multiple iterations of SGD similar to (3) on the global model θ^t using the public dataset D_p and obtains the model difference Δ_p . Then, the server selects a set of k coordinates with the largest absolute values in Δ_p and generates a corresponding mask vector \mathbf{m}^t (i.e., the procedure **SelectTopk**(\cdot)).

After receiving the global model θ^t and mask vector \mathbf{m}^t from the server, each client $i \in \mathcal{W}^t$ initializes its local model to θ^t and runs τ iterations of SGD to update its local model in parallel (lines 26-30). Then, the client i sparsifies its local model update $\theta^t - \theta_i^{t,\tau}$ using the mask vector \mathbf{m}^t (lines 33-37). Note that for rand_k sparsifier, the model update will be scaled by d/k to ensure an unbiased estimation on the sparsified model update (line 34). Since there is no a priori bound on the size of the sparsified model update Δ' , each client will clip its sparsified model update in ℓ_2 -norm with clipping threshold C so that $\|\hat{\Delta}\|_2 \leq C$ (line 38). Next, each client perturbs its sparsified model update by adding independent Gaussian noise $\mathcal{N}(0, C^2 \sigma^2 / r)$ on the k selected coordinates (line 39), where σ represents the noise multiplier. The noisy sparsified

model update Δ_i^t is then encrypted as an input into a secure aggregation protocol and sent to the server (line 32). Finally, the server computes the modular sum of all encrypted models to obtain the exact sum of local model updates $\sum_{i \in \mathcal{W}^t} \Delta_i^t$ and then updates the global model for the next round (line 13).

V. MAIN THEORETICAL RESULTS

In this section, we analyze the end-to-end privacy guarantee and convergence results of Fed-SMP. For better readability, we state the main theorems and only give the proof sketches in this section while leaving the full proofs to the appendix. Before presenting our theoretical results, we make the following assumptions:

Assumption 1 (Smoothness). *Each local objective function $f_i : \mathbb{R}^d \rightarrow \mathbb{R}$ is L -smooth, i.e., for any $\mathbf{x}, \mathbf{y} \in \mathbb{R}^d$,*

$$\|\nabla f_i(\mathbf{y}) - \nabla f_i(\mathbf{x})\| \leq L\|\mathbf{y} - \mathbf{x}\|, \forall i \in [n].$$

Assumption 2 (Unbiased Gradient and Bounded Variance). *The stochastic gradient at each client is an unbiased estimator of the local gradient: $\mathbb{E}[\mathbf{g}_i(\mathbf{x})] = \nabla f_i(\mathbf{x})$, and has bounded variance: $\mathbb{E}[\|\mathbf{g}_i(\mathbf{x}) - \nabla f_i(\mathbf{x})\|^2] \leq \zeta_i^2, \forall \mathbf{x} \in \mathbb{R}^d, i \in [n]$, where the expectation is over all the local mini-batches. We also denote $\bar{\zeta}^2 := (1/n) \sum_{i=1}^n \zeta_i^2$ for convenience.*

Assumption 3 (Bounded Dissimilarity). *There exist constants $\beta^2 \geq 1, \kappa^2 \geq 0$ such that $(1/n) \sum_{i=1}^n \|\nabla f_i(\mathbf{x})\|^2 \leq \beta^2 \|(1/n) \sum_{i=1}^n \nabla f_i(\mathbf{x})\|^2 + \kappa^2$. If local objective functions are identical to each other, then we have $\beta^2 = 1$ and $\kappa^2 = 0$.*

Assumptions 1 and 2 are standard in the analysis of SGD [25], and Assumption 3 is commonly used in the federated optimization literature [26], [27] to capture the dissimilarities of local objectives under non-IID data distribution.

A. Privacy Analysis

In this subsection, we provide the end-to-end privacy analysis of Fed-SMP based on RDP. Given the fact that the server only knows the sum of local model updates $\sum_{i \in \mathcal{W}^t} \Delta_i^t$ due to the use of secure aggregation, we need to compute the privacy loss incurred from releasing the sum of local model updates. Assume the client sets \mathcal{W} and \mathcal{W}' differ in one client index c such that $\mathcal{W}' := \mathcal{W} \cup \{c\}$. For any adjacent datasets $D := \{D_i\}_{i \in \mathcal{W}}$ and $D' := \{D_j\}_{j \in \mathcal{W}'} = \{D_i\}_{i \in \mathcal{W}} \cup D_c$, according to Definition 3, the ℓ_2 -sensitivity of the sum of local model updates is

$$\psi_\Delta := \sup_{D, D'} \left\| \sum_{i \in \mathcal{W}} \Delta_i^t(D_i) - \sum_{j \in \mathcal{W}'} \Delta_j^t(D_j) \right\|_2.$$

Due to the clipping, we have $\|\Delta_i^t(D_i)\|_2 \leq C, \forall i \in [n]$, and therefore $\psi_\Delta = \sup_{D, D'} \|\Delta_c^t(D_c)\|_2 \leq C$. As the sum of Gaussian random variables is still a Gaussian random variable, the variance of the Gaussian noise added to each selected coordinate of the sum of local model updates is $C^2\sigma^2$. According to Lemmas 1–4, we compute the overall privacy guarantee of Fed-SMP as follows:

Theorem 1 (Privacy Guarantee of Fed-SMP). *Suppose the client is sampled without replacement with probability $q := r/n$ at each round. For any $\epsilon < 2\log(1/\delta)$ and $\delta \in (0, 1)$, Fed-SMP satisfies (ϵ, δ) -DP after T communication rounds if*

$$\sigma^2 \geq \frac{7q^2T(\epsilon + 2\log(1/\delta))}{\epsilon^2}.$$

Proof. After adding noise $\mathcal{N}(0, C^2\sigma^2)$ to the k selected coordinates, the sum of local model updates satisfies $(\alpha, \alpha/2\sigma^2)$ -RDP for each client in \mathcal{W}^t at round t by Lemma 2. As r clients are uniformly sampled from all clients at each round, the per-round privacy guarantee of Fed-SMP can be further amplified according to the subsampling amplification property of RDP in Lemma 3. The overall privacy guarantee of Fed-SMP follows by using the composition property in Lemma 4 to compute the RDP guarantee after T rounds and Lemma 1 to convert RDP to (ϵ, δ) -DP. The details are given in Appendix D. \square

B. Convergence Analysis

In this subsection, we provide the convergence result of Fed-SMP under the general non-convex setting in Theorem 2.

Theorem 2 (Convergence result of Fed-SMP). *Under Assumptions 1–3, assume the local learning rate satisfies $\eta_l \leq \min\{(1/24\tau L(\phi_k + 1)\beta^2, 1/16\tau L\sqrt{8\beta^2 + 2}, 1/24\tau L\}$ and $\|\hat{\Delta}\|_2 \leq C$, then the sequence of outputs θ^t generated by Algorithm 1 satisfies:*

$$\begin{aligned} \frac{1}{T} \sum_{t=0}^{T-1} \|\nabla f(\theta^t)\|^2 &\leq \frac{8e_0}{T\eta_l\tau} + 8\eta_l\tau L(3\kappa^2 + 2\bar{\zeta}^2) \\ &+ (8\eta_l\tau L(2\kappa^2 + \bar{\zeta}^2) + \zeta')\phi_k + \frac{4LkC^2\sigma^2}{\eta_l\tau r^2}, \end{aligned} \quad (7)$$

where $e_0 := f(\theta^0) - f^*$, $\phi_k := 1 - k/d$ and $\zeta' := 4\bar{\zeta}^2/\gamma$ for top_k sparsifier, $\phi_k := d/k - 1$ and $\zeta' := 0$ for rand_k sparsifier, and f^* represents the optimal objective value.

Proof. The proof is given in Appendix E-F. \square

The convergence bound (7) contains three parts. The first two terms $8e_0/T\eta_l\tau + 8\eta_l\tau L(3\kappa^2 + 2\bar{\zeta}^2)$ represent the optimization error bound in FedAvg. The third term $(8\eta_l\tau L(2\kappa^2 + \bar{\zeta}^2) + \zeta')\phi_k$ is the *compression error* resulted from applying sparsification to compressing local model updates. The last term $4LkC^2\sigma^2/\eta_l\tau r^2$ is the *privacy error* resulted from adding DP noise to perturb local model updates. Both compression error and privacy error increase the error floor at convergence. When no sparsification is applied ($k = d$ and $\phi_k = 0$), the compression error becomes zero. When no DP noise is added ($\sigma = 0$), the privacy error becomes zero. The above result shows an explicit tradeoff between compression error and privacy error in Fed-SMP. As k decreases, the variance of sparsification ϕ_k gets larger, leading to a larger compression error, but the privacy error gets smaller. Therefore, there exists an optimal parameter k that can balance those two error terms to minimize the convergence bound.

VI. PERFORMANCE EVALUATION

In this section, we evaluate the performance of Fed-SMP with rand_k and top_k sparsifiers (denoted by Fed-SMP- rand_k and Fed-SMP- top_k , respectively) by comparing it with the following baselines:

- FedAvg: the classic non-private FL algorithm;
- FedAvg- top_k : a communication-efficient variant of FedAvg, where the local model update of each client is compressed using top_k sparsifier before being uploaded;
- FedAvg- rand_k : another communication-efficient variant of FedAvg, where the local model update of each client is compressed using rand_k sparsifier before being uploaded;
- DP-FedAvg [11]: a differentially-private variant of FedAvg, where the full-precision local model update from each client is clipped with clipping threshold C and then perturbed by adding Gaussian noise drawn from the distribution $\mathcal{N}(0, (C^2\sigma^2/r) \cdot \mathbf{I}_d)$, where σ is the noise multiplier and r is the number of selected clients per round.

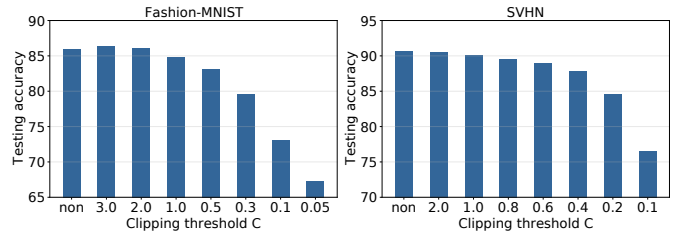
In the experiments, we compute the end-to-end privacy loss of DP-FedAvg and Fed-SMP using the API provided in [28].

A. Dataset and Model

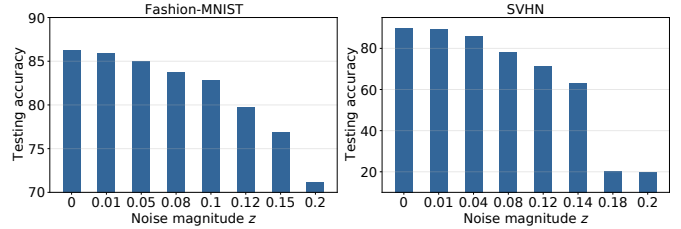
We conduct our experiments on Fashion-MNIST [29] dataset and extended SVHN dataset [30], two common benchmarks for differentially private machine learning. Note that while these two datasets are considered as “solved” in the computer vision community, achieving high accuracy with strong privacy guarantee remains difficult on these datasets [31].

The Fashion-MNIST dataset consists of a training set of 60,000 examples and a test set of 10,000 examples. Each example is a 28×28 grayscale image associated with a label from 10 classes. For Fed-SMP- top_k , we randomly sample 1,000 examples from the training set as the public dataset D_p and evenly partition the remaining 59,000 examples across 6,000 clients. For other algorithms, we evenly split the training data across 6,000 clients. We use the convolutional neural network (CNN) model in [5] on Fashion-MNIST that consists of two 5×5 convolution layers (the first with 32 filters, the second with 64 filters, each followed with 2×2 max pooling and ReLu activation), a fully connected layer with 512 units and ReLu activation, and a final softmax output later, which results in about 1.6 million total parameters.

The SVHN dataset contains 73,257 training examples and 26,032 testing examples, and each of them is a 32×32 colored image of digits from 0 to 9. We extend the training set with another 531,131 additional examples. For all algorithms except Fed-SMP- top_k , we evenly partition the training set across 6,000 clients. For Fed-SMP- top_k , we randomly sample 2,000 examples from the training set as the public dataset D_p and evenly partition the remaining across 6,000 clients. We train a CNN model used in [32] on SVHN dataset, which stacks two 5×5 convolution layers (the first with 64 filters, the second with 128 filters, each followed with 2×2 max pooling and



(a) Impact of clipping threshold C .



(b) Impact of noise magnitude z .

Figure 2: Impacts of model update clipping threshold C and noise magnitude z on model accuracy of FedAvg after 180 communication rounds.

ReLU activation), two fully connected layers (the first with 384 units, the second with 192 units, each followed with ReLu activation), and a final softmax output later, resulting in about 3.4 million parameters in total.

B. Experimental Settings

For both datasets, at each communication round, the server randomly samples $r = 100$ clients to participate in the training. For the local optimizer on clients, we use momentum SGD for both datasets. Specifically, for Fashion-MNIST, we set the local momentum coefficient as 0.5, local learning rate as $\eta_l = 0.125$ decaying at a rate of 0.99 at each communication round, batch size $B = 10$ and local update period to be 10 epochs; for SVHN, we set the local momentum coefficient as 0.8, local learning rate as $\eta_l = 0.05$ decaying at a rate of 0.99 at each communication round, batch size $B = 50$ and local update period to be 5 epochs. It is worth noting that the momentum at each client is initialized at the beginning of every communication round, since local momentum will be stale due to the partial participation of clients. Specially, for Fed-SMP- top_k , the server uses the same optimizer as the clients with the same local update period to compute the global model update Δ_p .

In all privacy-preserving algorithms, we set $\delta = 10^{-4}$ such that δ is much less than $1/n$ and $\epsilon = 1.0$ in the end-to-end (ϵ, δ) -DP guarantee after $T = 180$ rounds. To select the clipping threshold C , we investigate its impact on the convergence of FedAvg after 180 communication rounds for both datasets. From Figure 2a, we find that choosing $C \in [1, 3]$ has a minimal impact on the model accuracy of Fashion-MNIST dataset, and choosing $C \in [0.4, 2.0]$ has a minimal impact on the model accuracy of SVHN dataset. To choose the noise multiplier σ , we evaluate the impact of various levels

Compression ratio	Algorithm	Performance		
		Testing Accuracy (%)	Uplink Communication Cost (MB)	Privacy Loss (ϵ)
$p = 0.001$	Fed-SMP-top $_k$	77.18 ± 0.48	0.02	1.0
	Fed-SMP-rand $_k$	27.16 ± 10.20	0.02	1.0
$p = 0.005$	Fed-SMP-top $_k$	80.76 ± 0.27	0.10	1.0
	Fed-SMP-rand $_k$	56.04 ± 5.22	0.10	1.0
$p = 0.01$	Fed-SMP-top $_k$	80.76 ± 0.47	0.20	1.0
	Fed-SMP-rand $_k$	65.61 ± 1.04	0.20	1.0
$p = 0.1$	Fed-SMP-top $_k$	80.49 ± 0.23	2.00	1.0
	Fed-SMP-rand $_k$	77.59 ± 0.53	2.00	1.0
$p = 0.2$	Fed-SMP-top $_k$	80.16 ± 0.09	3.99	1.0
	Fed-SMP-rand $_k$	79.12 ± 0.40	3.99	1.0
$p = 0.4$	Fed-SMP-top $_k$	80.26 ± 0.25	7.98	1.0
	Fed-SMP-rand $_k$	79.88 ± 0.37	7.98	1.0
$p = 0.8$	Fed-SMP-top $_k$	79.77 ± 1.00	15.97	1.0
	Fed-SMP-rand $_k$	79.82 ± 0.35	15.97	1.0
$p = 1.0$	DP-FedAvg	72.72 ± 3.72	19.96	1.0
	FedAvg	86.98 ± 0.12	19.96	-

Table I: Summary of results on Fashion-MNIST dataset.

Compression ratio	Algorithm	Performance		
		Testing accuracy (%)	Uplink Communication Cost (MB)	Privacy loss (ϵ)
$p = 0.005$	Fed-SMP-top $_k$	80.94 ± 0.85	0.21	1.0
	Fed-SMP-rand $_k$	19.45 ± 0.42	0.21	1.0
$p = 0.01$	Fed-SMP-top $_k$	81.12 ± 1.08	0.41	1.0
	Fed-SMP-rand $_k$	19.75 ± 0.12	0.41	1.0
$p = 0.05$	Fed-SMP-top $_k$	80.22 ± 1.02	2.06	1.0
	Fed-SMP-rand $_k$	28.15 ± 2.46	2.06	1.0
$p = 0.1$	Fed-SMP-top $_k$	79.64 ± 0.29	4.12	1.0
	Fed-SMP-rand $_k$	64.50 ± 2.95	4.12	1.0
$p = 0.2$	Fed-SMP-top $_k$	77.91 ± 0.37	8.24	1.0
	Fed-SMP-rand $_k$	76.94 ± 0.58	8.24	1.0
$p = 0.4$	Fed-SMP-top $_k$	75.58 ± 0.40	16.47	1.0
	Fed-SMP-rand $_k$	77.07 ± 0.48	16.47	1.0
$p = 0.8$	Fed-SMP-top $_k$	73.18 ± 0.69	32.94	1.0
	Fed-SMP-rand $_k$	73.90 ± 0.37	32.94	1.0
$p = 1.0$	DP-FedAvg	72.46 ± 0.54	41.18	1.0
	FedAvg	88.47 ± 0.17	41.18	-

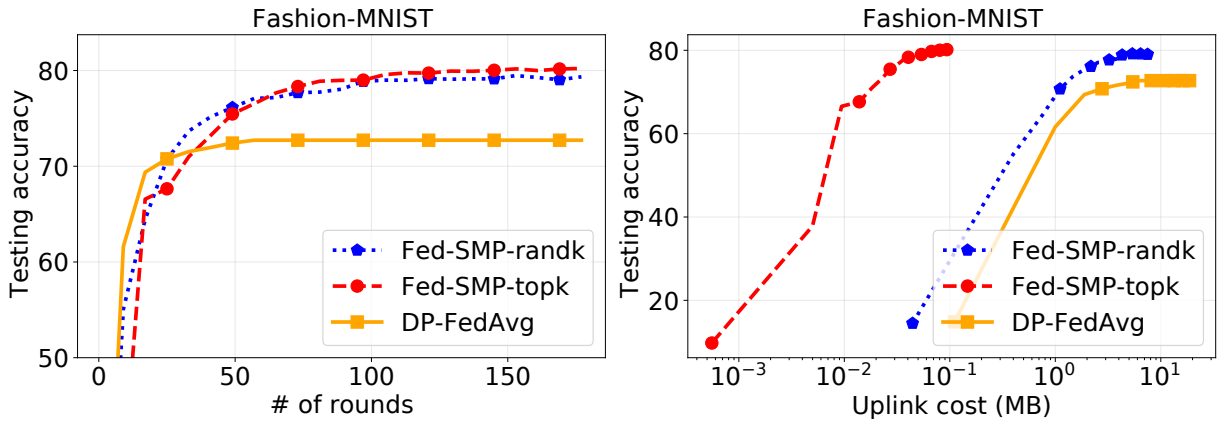
Table II: Summary of results on SVHN dataset.

of per-coordinate Gaussian noise $\mathcal{N}(0, C^2\sigma^2/r)$ added to the local model update while setting $C = 3$ for Fashion-MNIST dataset and $C = 2$ for SVHN dataset. Let $z := C\sigma/\sqrt{r}$ denote the noise magnitude. As shown in Figure 2b, we can see that a small decrease in model accuracy when the noise magnitude z varies between 0.01 and 0.15 for Fashion-MNIST dataset and between 0.01 and 0.08 for SVHN dataset. With the above observations, we fix $C = 1$ and $\sigma = 1.4$ for all experiments on Fashion-MNIST dataset, and $C = 0.4$ and $\sigma = 1.4$ for all experiments on SVHN dataset. In addition, we define the *compression ratio* for rand $_k$ and top $_k$ sparsifiers as $p = k/d$. When p is smaller, more coordinates of the local model updates are set to zero, leading to a higher level of

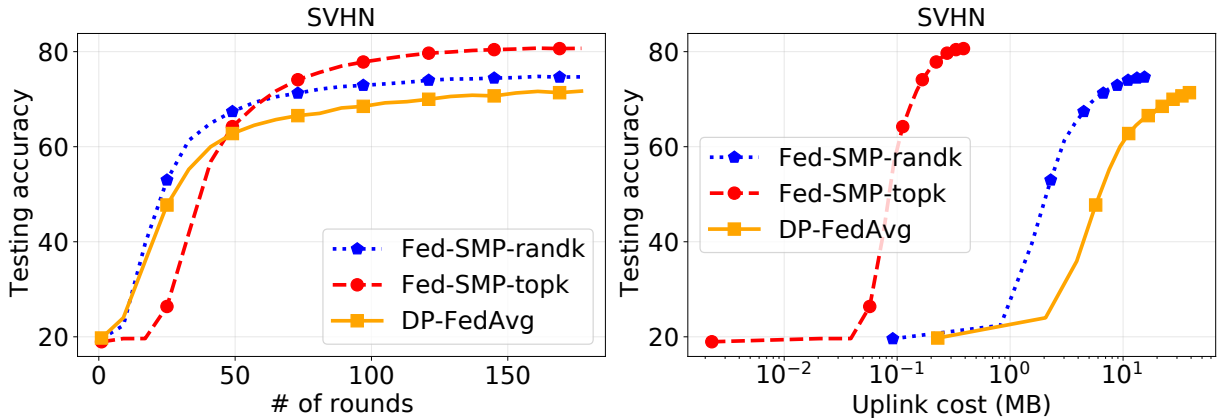
communication compression.

C. Experiment Results

Table I and Table II summarize the performance of FedAvg, DP-FedAvg and Fed-SMP after T rounds on Fashion-MNIST dataset and SVHN dataset, respectively. We run each experiment with 5 random seeds and report the average and standard deviation of *testing accuracy*. Note that we always report the best testing accuracy across all rounds in each experiment. The *uplink communication cost* denotes the size of the data sent from a client to the server as the input into the secure aggregation protocol, which equals to $32k \times T \times (r/n)$ bits for Fed-SMP and $32d \times T \times (r/n)$ bits for DP-FedAvg and



(a) Fashion-MNIST dataset.



(b) SVHN dataset.

Figure 3: Testing accuracy of Fed-SMP and DP-FedAvg w.r.t. communication round (left) and uplink communication cost (right).

FedAvg. The *privacy loss* for DP-FedAvg and Fed-SMP is the accumulated privacy loss ϵ at the end of the training.

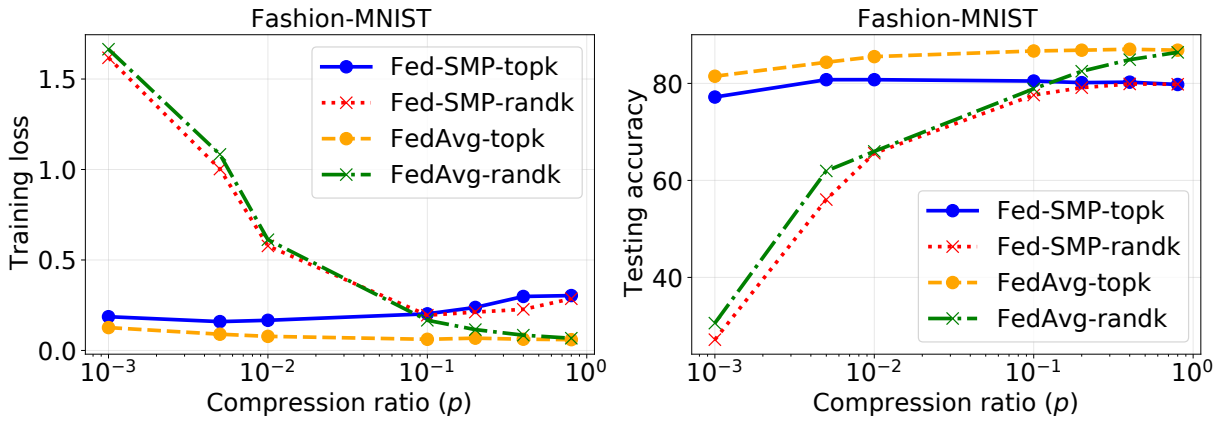
From Table I, we can see that the non-private FedAvg achieves a testing accuracy of 86.61% on Fashion-MNIST dataset. When adding Gaussian noise to ensure $(1, 10^{-4})$ -DP, the accuracy drops to 71.40% for DP-FedAvg. By choosing a proper value of p , Fed-SMP can reach a higher accuracy than DP-FedAvg under the same level of DP guarantee. For example, the highest testing accuracy of Fed-SMP-top_k is 80.76% when $p = 0.005$, outperforming DP-FedAvg by 11%; the highest testing accuracy of Fed-SMP-rand_k is 79.88% when $p = 0.4$, outperforming DP-FedAvg by 10%.

From Table II, we can see that the accuracy of non-private FedAvg on SVHN dataset is 88.47%, and then it decreases to 72.46% to achieve $(1, 10^{-4})$ -DP guarantee for DP-FedAvg. For Fed-SMP with the same level of DP guarantee, Fed-SMP-top_k can achieve a testing accuracy of 81.12% on SVHN dataset when $p = 0.01$, outperforming DP-FedAvg by 12%, and Fed-SMP-rand_k can achieve a testing accuracy of 77.07% on SVHN dataset when $p = 0.4$, outperforming DP-FedAvg by 6%.

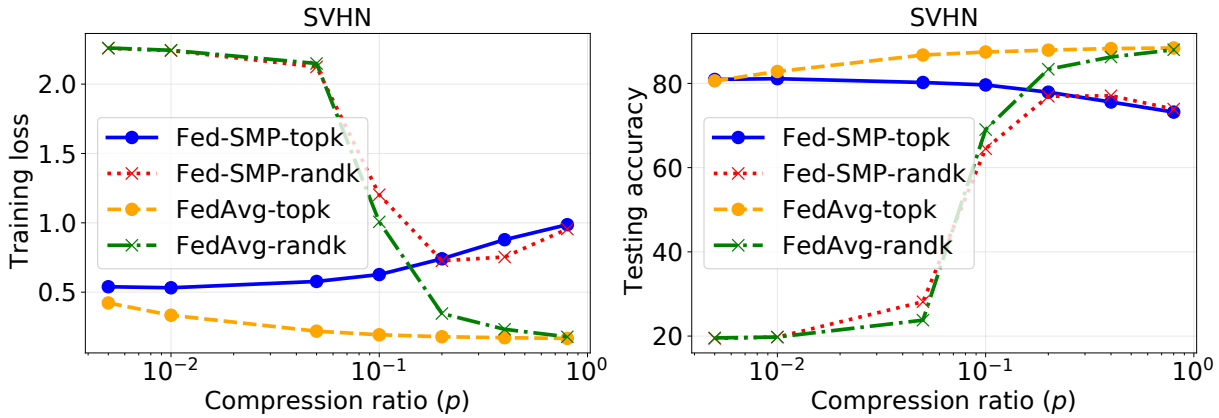
In the following, we will further evaluate Fed-SMP with more experimental settings.

1) *Communication efficiency of Fed-SMP*: For the communication cost, we can observe from Table I and Table II that the uplink communication cost for Fed-SMP on both datasets is relatively lower than that of DP-FedAvg under the same privacy guarantee, since our scheme integrates well with the secure aggregation protocol and takes advantage of model update compression. To further demonstrate the communication efficiency of Fed-SMP, we show the convergence speed and communication cost of our Fed-SMP algorithms. Specifically, we select the Fed-SMP algorithms with the optimal compression ratio and show its testing accuracy with respect to the communication round and uplink communication cost: For Fashion-MNIST dataset, we draw the results of Fed-SMP-top_k with $p = 0.005$ and Fed-SMP-rand_k with $p = 0.4$ in Figure 3a, compared with DP-FedAvg; for SVHN dataset, we draw the results of Fed-SMP-top_k with $p = 0.01$ and Fed-SMP-rand_k with $p = 0.4$ in Figure 3b, compared with DP-FedAvg.

As shown in Figure 3a, for Fashion-MNIST dataset, Fed-



(a) Fashion-MNIST dataset.



(b) SVHN dataset.

Figure 4: Training loss and testing accuracy of Fed-SMP w.r.t compression ratio, compared with FedAvg with $\text{rand}_k/\text{top}_k$.

SMP- top_k and Fed-SMP- rand_k converge slower than DP-FedAvg due to the use of sparsification. However, the final accuracy of Fed-SMP is higher than DP-FedAvg because of the advantage of sparsification in improving privacy and model accuracy. Moreover, we find that Fed-SMP is more communication-efficient than DP-FedAvg, and Fed-SMP- top_k is more communication-efficient than Fed-SMP- rand_k . For instance, to achieve a target accuracy 72% on Fashion-MNIST dataset, Fed-SMP- top_k and Fed-SMP- rand_k save 99% and 70% of uplink communication cost compared with DP-FedAvg, respectively. For SVHN dataset in Figure 3b, even though sparsification will slow down the convergence, both Fed-SMP- top_k and Fed-SMP- rand_k converge faster than DP-FedAvg because of the significant privacy benefit of sparsification, so that Fed-SMP- top_k and Fed-SMP- rand_k finally achieve higher accuracies than DP-FedAvg under the same $(1, 10^{-4})$ -DP guarantee. Similar to Fashion-MNIST dataset, Fed-SMP also demonstrates its advantage in saving communication cost on SVHN dataset: to achieve a target accuracy 72% on SVHN dataset, Fed-SMP- top_k and Fed-SMP- rand_k save 99% and 82% of uplink communication cost compared with DP-FedAvg, respectively.

2) *Tradeoff between privacy and compression errors*: From Table I and Table II, we have observed that as p decreases from 1.0 to a small value (e.g., 0.005), the testing accuracy of Fed-SMP first increases and then decreases. This is due to the change of privacy error and compression error in the convergence bound (7), which is controlled by the compression ratio p . In the following, we conduct additional experiments to further demonstrate this tradeoff under various compression ratios. As it is hard to directly show the tradeoff between privacy error and compression error, we study the difference between the performances of Fed-SMP and FedAvg- $\text{rand}_k/\text{top}_k$, which differ only in DP noise addition.

Specifically, we show the training losses and testing accuracies of Fed-SMP, FedAvg- rand_k and FedAvg- top_k on Fashion-MNIST dataset (Figure 4a) and SVHN dataset (Figure 4b) with respect to different compression ratios. We can see that as the compression ratio p increases, the training losses of FedAvg- rand_k and FedAvg- top_k on both datasets monotonically decrease, and the corresponding testing accuracies monotonically increase, due to the decreasing compression error incurred from sparsification. However, the training losses of Fed-SMP- rand_k and Fed-SMP- top_k decrease at first and

then increase, and the corresponding testing accuracies increase at first and then decrease. This matches our observations from Theorem 2, i.e., the performance of Fed-SMP depends on the tradeoff between the compression error and privacy error. When p is too small (e.g., $p < 0.1$ for Fed-SMP- rand_k on both datasets), despite of the privacy amplification effect of compression that reduces the amount of added Gaussian noise, the compression error is large and dominates the total convergence error, leading to a higher training loss and lower testing accuracy. As p increases, the compression error decreases, leading to a lower training loss. However, if p becomes too large, the privacy amplification effect of compression becomes negligible, and the privacy error starts to dominate the convergence error, leading to a higher training loss. For example, the testing accuracies of Fed-SMP- rand_k on both datasets start to decrease when $p > 0.4$, and the testing accuracy of Fed-SMP- top_k starts to decrease when $p > 0.005$ on Fashion-MNIST dataset and $p > 0.01$ on SVHN dataset. Therefore, to achieve the best performance of Fed-SMP, the choice of p needs to balance the privacy error and compression error. Furthermore, we find that Fed-SMP- top_k tends to achieve its best performance when p is small (i.e., 0.005 and 0.01 for Fashion-MNIST and SVHN datasets, respectively), and Fed-SMP- rand_k tends to achieve its best performance when p is large (i.e., 0.4 on both datasets).

VII. RELATED WORK

FL, or distributed learning in general, with DP has attracted increasing attentions recently. Different from centralized learning, FL involves multiple communication rounds between clients and the server, and therefore DP needs to be preserved for all communication rounds. The main challenge of achieving DP in FL lies in maintaining high model accuracy under reasonable DP guarantee. Prior related works rely on specialized techniques such as shuffling [12], [13], [33] and aggregation directly over wireless channels [34] to boost DP guarantee with the same amount of noise, which are only applicable to some specific settings. Our approach is orthogonal to theirs and can be combined to achieve even better privacy-accuracy tradeoffs. Some works [35], [36] also develop differentially private versions of distributed algorithms that require fewer iterations than SGD-based algorithms to converge such as alternating direction method of multipliers, but they are only applicable to convex setting and do not allow partial client participation at each communication round, which is a key feature in FL.

Client-level DP provides more realistic protections than record-level DP against information leakage in the FL setting. With client-level DP, the participation of a client rather than a single data record needs to be protected, therefore requiring the addition of a larger amount of noise than record-level DP to achieve the same level of DP [11], [37]. Our work follows this line of research and proposes to integrate SMP with FedAvg to achieve higher model accuracy than prior schemes under the same client-level DP guarantee in FL. Note there are also other approaches of preserving privacy in distributed learning,

such as secure multi-party computation [38] or homomorphic encryption [39]. However, those approaches have a different privacy goal and cannot protect information leakage incurred from observing the final trained models at the server.

Besides privacy, another bottleneck in FL is the high communication cost of transmitting model parameters. Typical techniques to address this issue include quantization [40], [41] and sparsification [42]. However, they do not consider the privacy aspect. Some recent works [43]–[45] have started to jointly consider communication efficiency and DP in distributed learning. Agarwal et al. [43] propose cpSGD by making modifications to distributed SGD to make the method both private and communication-efficient. However, the authors treat these as separate issues and develop different approaches to address each within cpSGD. As shown in [46], by separately reducing communication and enforcing privacy, errors in cpSGD are compounded and higher than considering privacy only. In comparison, our proposed Fed-SMP scheme considers those two issues jointly and provides substantially higher accuracy by leveraging sparsification to amplify privacy protection. Zhang et al. [44] also combine sparsification with Gaussian mechanism to achieve communication efficiency and DP in decentralized SGD, but their scheme adds noise before using sparsification and cannot leverage sparsification to improve privacy protection. Kerkouche et al. [45] proposes to use compressive sensing before adding noise to model updates in FL but relies on the strong assumption that model updates only have a few non-zero coordinates, which seldom holds in practice.

VIII. CONCLUSIONS

This paper has proposed Fed-SMP, a new FL scheme based on sparsified model perturbation. Fed-SMP achieves client-level DP while maintaining high model accuracy and is also communication-efficient. We have rigorously analyzed the convergence and end-to-end DP guarantee of the proposed scheme and extensively evaluated its performance on two common benchmark datasets. Experimental results have shown that Fed-SMP with both rand_k and top_k sparsification strategies can improve the privacy-accuracy tradeoff and communication efficiency simultaneously compared with the existing methods. In the future, we will consider other compression methods such as low-rank approximation and quantization, and extend the scheme to alternative FL settings such as shuffled model.

REFERENCES

- [1] A. Pothitos, “IoT and wearables: Fitness tracking,” 2017, <http://www.mobileindustryreview.com/2017/03/iot-wearables-fitness-tracking.html>.
- [2] P. Goldstein, “Smart cities gain efficiencies from IoT traffic sensors and data,” 2018, <https://statetechmagazine.com/article/2018/12/smart-cities-gain-efficiencies-iot-traffic-sensors-and-data-perfcon>.
- [3] A. Weinreic, “The future of the smart home: Smart homes and IoT: A century in the making,” 2018, <https://statetechmagazine.com/article/2018/12/smart-cities-gain-efficiencies-iot-traffic-sensors-and-data-perfcon>.
- [4] P. Kairouz, H. B. McMahan, B. Avent, A. Bellet, M. Bennis, A. N. Bhagoji, K. Bonawitz, Z. Charles, G. Cormode, R. Cummings *et al.*, “Advances and open problems in federated learning,” *Foundations and Trends® in Machine Learning*, vol. 14, no. 1–2, pp. 1–210, 2021.

- [5] B. McMahan, E. Moore, D. Ramage, S. Hampson, and B. A. y Arcas, "Communication-efficient learning of deep networks from decentralized data," in *Artificial Intelligence and Statistics*, 2017, pp. 1273–1282.
- [6] R. Shokri, M. Stronati, C. Song, and V. Shmatikov, "Membership inference attacks against machine learning models," in *IEEE Symposium on Security and Privacy (SP)*. IEEE, 2017, pp. 3–18.
- [7] M. Fredrikson, S. Jha, and T. Ristenpart, "Model inversion attacks that exploit confidence information and basic countermeasures," in *Proceedings of the 22nd ACM SIGSAC Conference on Computer and Communications Security*. ACM, 2015, pp. 1322–1333.
- [8] C. Dwork, A. Roth *et al.*, "The algorithmic foundations of differential privacy," *Foundations and Trends® in Theoretical Computer Science*, vol. 9, no. 3–4, pp. 211–407, 2014.
- [9] R. C. Geyer, T. Klein, and M. Nabi, "Differentially private federated learning: A client level perspective," *arXiv preprint arXiv:1712.07557*, 2018.
- [10] M. Abadi, A. Chu, I. Goodfellow, H. B. McMahan, I. Mironov, K. Talwar, and L. Zhang, "Deep learning with differential privacy," in *Proceedings of the ACM SIGSAC Conference on Computer and Communications Security*, 2016, pp. 308–318.
- [11] H. B. McMahan, D. Ramage, K. Talwar, and L. Zhang, "Learning differentially private recurrent language models," in *International Conference on Learning Representations*, 2018.
- [12] R. Liu, Y. Cao, H. Chen, R. Guo, and M. Yoshikawa, "FLAME: Differentially private federated learning in the shuffle model," in *Proceedings of the AAAI Conference on Artificial Intelligence*, 2021.
- [13] Ú. Erlingsson, V. Feldman, I. Mironov, A. Raghunathan, K. Talwar, and A. Thakurta, "Amplification by shuffling: From local to central differential privacy via anonymity," in *Proceedings of the Thirtieth Annual ACM-SIAM Symposium on Discrete Algorithms*. SIAM, 2019, pp. 2468–2479.
- [14] I. Mironov, "Rényi differential privacy," in *2017 IEEE 30th Computer Security Foundations Symposium (CSF)*. IEEE, 2017, pp. 263–275.
- [15] Y. Wang, B. Balle, and S. P. Kasiviswanathan, "Subsampled rényi differential privacy and analytical moments accountant," in *The 22nd International Conference on Artificial Intelligence and Statistics*. PMLR, 2019, pp. 1226–1235.
- [16] L. Wang, B. Jayaraman, D. Evans, and Q. Gu, "Efficient privacy-preserving nonconvex optimization," *arXiv preprint arXiv:1910.13659*, 2020.
- [17] K. Bonawitz, H. Eichner, W. Grieskamp, D. Huba, A. Ingerman, V. Ivanov, C. Kiddon, J. Konečný, S. Mazzocchi, B. McMahan, T. Van Overveldt, D. Petrou, D. Ramage, and J. Roselander, "Towards federated learning at scale: System design," in *Proceedings of Machine Learning and Systems*, vol. 1, 2019, pp. 374–388.
- [18] K. Bonawitz, V. Ivanov, B. Kreuter, A. Marcedone, H. B. McMahan, S. Patel, D. Ramage, A. Segal, and K. Seth, "Practical secure aggregation for privacy-preserving machine learning," in *Proceedings of the 2017 ACM SIGSAC Conference on Computer and Communications Security*, 2017, pp. 1175–1191.
- [19] S. Goryczka, L. Xiong, and V. Sunderam, "Secure multiparty aggregation with differential privacy: A comparative study," in *Proceedings of the Joint EDBT/ICDT 2013 Workshops*, 2013, pp. 155–163.
- [20] S. Truex, N. Baracaldo, A. Anwar, T. Steinke, H. Ludwig, R. Zhang, and Y. Zhou, "A hybrid approach to privacy-preserving federated learning," in *Proceedings of the 12th ACM Workshop on Artificial Intelligence and Security*, 2019, pp. 1–11.
- [21] F. Valovich and F. Alda, "Computational differential privacy from lattice-based cryptography," in *International Conference on Number-Theoretic Methods in Cryptology*. Springer, 2017, pp. 121–141.
- [22] K. Bonawitz, F. Salehi, J. Konečný, B. McMahan, and M. Gruteser, "Federated learning with autotuned communication-efficient secure aggregation," in *2019 53rd Asilomar Conference on Signals, Systems, and Computers*. IEEE, 2019, pp. 1222–1226.
- [23] N. Papernot, S. Song, I. Mironov, A. Raghunathan, K. Talwar, and Ú. Erlingsson, "Scalable private learning with PATE," in *International Conference on Learning Representations*, 2018.
- [24] J. Wang and Z.-H. Zhou, "Differentially private learning with small public data," in *Proceedings of the AAAI Conference on Artificial Intelligence*, vol. 34, no. 04, 2020, pp. 6219–6226.
- [25] L. Bottou, F. E. Curtis, and J. Nocedal, "Optimization methods for large-scale machine learning," *SIAM Review*, vol. 60, no. 2, pp. 223–311, 2018.
- [26] R. Ward, X. Wu, and L. Bottou, "AdaGrad stepsizes: Sharp convergence over nonconvex landscapes," in *International Conference on Machine Learning*. PMLR, 2019, pp. 6677–6686.
- [27] X. Li, K. Huang, W. Yang, S. Wang, and Z. Zhang, "On the convergence of FedAvg on Non-IID data," in *International Conference on Learning Representations*, 2020.
- [28] "Opacus PyTorch library," Available from <https://opacus.ai>.
- [29] H. Xiao, K. Rasul, and R. Vollgraf, "Fashion-MNIST: a novel image dataset for benchmarking machine learning algorithms," *arXiv preprint arXiv:1708.07747*, 2017.
- [30] Y. Netzer, T. Wang, A. Coates, A. Bissacco, B. Wu, and A. Y. Ng, "Reading digits in natural images with unsupervised feature learning," in *NeurIPS Workshop on Deep Learning and Unsupervised Feature Learning*, 2011.
- [31] N. Papernot, A. Thakurta, S. Song, S. Chien, and U. Erlingsson, "Tempered sigmoid activations for deep learning with differential privacy," in *Proceedings of the AAAI Conference on Artificial Intelligence*, vol. 35, no. 10, 2021, pp. 9312–9321.
- [32] Z. Liang, B. Wang, Q. Gu, S. Osher, and Y. Yao, "Exploring private federated learning with laplacian smoothing," *arXiv preprint arXiv:2005.00218*, 2021.
- [33] A. Girgis, D. Data, S. Diggavi, P. Kairouz, and A. T. Suresh, "Shuffled model of differential privacy in federated learning," in *International Conference on Artificial Intelligence and Statistics*. PMLR, 2021, pp. 2521–2529.
- [34] M. Seif, R. Tandon, and M. Li, "Wireless federated learning with local differential privacy," in *2020 IEEE International Symposium on Information Theory (ISIT)*. IEEE, 2020, pp. 2604–2609.
- [35] Y. Guo and Y. Gong, "Practical collaborative learning for crowdsensing in the internet of things with differential privacy," in *2018 IEEE Conference on Communications and Network Security (CNS)*. IEEE, 2018, pp. 1–9.
- [36] Z. Huang, R. Hu, Y. Guo, E. Chan-Tin, and Y. Gong, "DP-ADMM: ADMM-based distributed learning with differential privacy," *IEEE Transactions on Information Forensics and Security*, vol. 15, pp. 1002–1012, 2019.
- [37] K. Wei, J. Li, M. Ding, C. Ma, H. Su, B. Zhang, and H. V. Poor, "User-level privacy-preserving federated learning: Analysis and performance optimization," *IEEE Transactions on Mobile Computing*, 2021.
- [38] R. Kanagavelu, Z. Li, J. Samsudin, Y. Yang, F. Yang, R. S. M. Goh, M. Cheah, P. Wiwatphonthana, K. Akkarajitsakul, and S. Wang, "Two-phase multi-party computation enabled privacy-preserving federated learning," in *20th IEEE/ACM International Symposium on Cluster, Cloud and Internet Computing (CCGRID)*. IEEE, 2020, pp. 410–419.
- [39] Y. Aono, T. Hayashi, L. Wang, S. Moriai *et al.*, "Privacy-preserving deep learning via additively homomorphic encryption," *IEEE Transactions on Information Forensics and Security*, vol. 13, no. 5, pp. 1333–1345, 2017.
- [40] D. Alistarh, D. Grubic, J. Li, R. Tomioka, and M. Vojnovic, "QSGD: Communication-efficient SGD via gradient quantization and encoding," in *Advances in Neural Information Processing Systems*, 2017, pp. 1709–1720.
- [41] J. Bernstein, Y.-X. Wang, K. Azzadenesheli, and A. Anandkumar, "signSGD: Compressed optimisation for non-convex problems," in *International Conference on Machine Learning*. PMLR, 2018, pp. 560–569.
- [42] H. Wang, S. Sievert, S. Liu, Z. Charles, D. Papailiopoulos, and S. Wright, "Atomo: Communication-efficient learning via atomic sparsification," in *Advances in Neural Information Processing Systems*, 2018, pp. 9850–9861.
- [43] N. Agarwal, A. T. Suresh, F. X. X. Yu, S. Kumar, and B. McMahan, "cpSGD: Communication-efficient and differentially-private distributed SGD," in *Advances in Neural Information Processing Systems*, 2018, pp. 7564–7575.
- [44] X. Zhang, M. Fang, J. Liu, and Z. Zhu, "Private and communication-efficient edge learning: A sparse differential gaussian masking distributed SGD approach," in *Proceedings of the Twenty-First International Symposium on Theory, Algorithmic Foundations, and Protocol Design for Mobile Networks and Mobile Computing*, 2020, pp. 261–270.
- [45] R. Kerkouche, G. Ács, C. Castelluccia, and P. Genevès, "Compression boosts differentially private federated learning," in *6th IEEE European Symposium on Security and Privacy*, 2021.
- [46] T. Li, Z. Liu, V. Sekar, and V. Smith, "Privacy for free: Communication-efficient learning with differential privacy using sketches," *arXiv preprint arXiv:1911.00972*, 2019.

A. Notations

For ease of expression, let $\theta_i^{t,s}$ denote client i 's local model at local iteration s of round t , and let \mathbf{b}_i^t denote the Gaussian noise added to the sparsified model update where $[\mathbf{b}_i^t]_j \sim \mathcal{N}(0, C^2\sigma^2/r)$ if $j \in \mathcal{V}^t$ and $[\mathbf{b}_i^t]_j = 0$ otherwise. Let spar denote the sparsifier. In Fed-SMP, the update rule of the global model can be summarized as:

$$\boldsymbol{\theta}^{t+1} = \boldsymbol{\theta}^t - \frac{1}{r} \sum_{i \in \mathcal{W}^t} \Delta_i^t, \quad \text{where } \Delta_i^t = \text{spar}(\eta_l \sum_{s=0}^{\tau-1} \mathbf{g}_i^{t,s}) + \mathbf{b}_i^t \quad (8)$$

where Δ_i^t represents the sparsified noisy model update of client i . Assume the clients are sampled uniformly at random without replacement, then we can directly validate that the client sampling is unbiased:

$$\mathbb{E}_{\mathcal{W}^t} \left[\frac{1}{r} \sum_{i \in \mathcal{W}^t} \Delta_i^t \right] = \frac{1}{r} \sum_{\substack{\mathcal{W} \in [n], \\ |\mathcal{W}|=r}} \mathbb{P}(\mathcal{W}^t = \mathcal{W}) \sum_{i \in \mathcal{W}^t} \Delta_i^t = \frac{1}{n} \sum_{i=1}^n \Delta_i^t. \quad (9)$$

Moreover, let $\nabla f_i(\boldsymbol{\theta}_i^{t,s})$ represent the local gradient so that $\mathbb{E}_{\mathcal{E}_i^{t,s}}[\mathbf{g}_i^{t,s}] = \nabla f_i(\boldsymbol{\theta}_i^{t,s})$. For ease of expression, we let $\mathbf{d}_i^t = (1/\tau) \sum_{s=0}^{\tau-1} \mathbf{g}_i^{t,s}$ and $\mathbf{h}_i^t = (1/\tau) \sum_{s=0}^{\tau-1} \nabla f_i(\boldsymbol{\theta}_i^{t,s})$, so we have $\Delta_i^t = \eta_l \tau \text{spar}(\mathbf{d}_i^t) + \mathbf{b}_i^t$ and $\mathbb{E}_t[\mathbf{d}_i^t] = \mathbf{h}_i^t$.

B. Useful Inequalities

Lemma 5 (Jensen's inequality). *For arbitrary set of n vectors $\{\mathbf{a}_i\}_{i=1}^n, \mathbf{a}_i \in \mathbb{R}^d$ and positive weights $\{w_i\}_{i \in [n]}$,*

$$\left\| \sum_{i=1}^n w_i \mathbf{a}_i \right\|^2 \leq \frac{\sum_{i=1}^n w_i \|\mathbf{a}_i\|^2}{\sum_{i=1}^n w_i}. \quad (10)$$

Lemma 6. *For arbitrary set of n vectors $\{\mathbf{a}_i\}_{i=1}^n, \mathbf{a}_i \in \mathbb{R}^d$,*

$$\left\| \sum_{i=1}^n \mathbf{a}_i \right\|^2 \leq n \sum_{i=1}^n \|\mathbf{a}_i\|^2. \quad (11)$$

Lemma 7. *For given two vectors $\mathbf{a}, \mathbf{b} \in \mathbb{R}^d$,*

$$\|\mathbf{a} + \mathbf{b}\|^2 \leq (1 + \alpha)\|\mathbf{a}\|^2 + (1 + \alpha^{-1})\|\mathbf{b}\|^2, \forall \alpha > 0. \quad (12)$$

Lemma 8. *For given two vectors $\mathbf{a}, \mathbf{b} \in \mathbb{R}^d$,*

$$2\langle \mathbf{a}, \mathbf{b} \rangle \leq \gamma\|\mathbf{a}\|^2 + \gamma^{-1}\|\mathbf{b}\|^2, \forall \gamma > 0. \quad (13)$$

C. Intermediate Results

Lemma 9 (Bounded Sparsification). *Given a vector $\mathbf{x} \in \mathbb{R}^d$, parameter $k \in [d]$. The sparsifier $\{\text{rand}_k(\mathbf{x}), \text{top}_k(\mathbf{x})\}$ holds that*

$$\mathbb{E} \|\text{top}_k(\mathbf{x}) - \mathbf{x}\|^2 \leq \left(1 - \frac{k}{d}\right) \|\mathbf{x}\|^2; \quad \mathbb{E} \left\| \frac{d}{k} \text{rand}_k(\mathbf{x}) - \mathbf{x} \right\|^2 \leq \left(\frac{d}{k} - 1\right) \|\mathbf{x}\|^2$$

Proof. For the rand_k sparsifier, by applying the expectation over the active set ω , we have

$$\mathbb{E}_{\omega} \left[\frac{d}{k} \text{rand}_k(\mathbf{x}) \right] = \frac{d}{k} \left[\frac{k}{d} [\mathbf{x}]_1, \dots, \frac{k}{d} [\mathbf{x}]_d \right] = \mathbf{x},$$

$$\begin{aligned} \mathbb{E}_{\omega} \|\text{rand}_k(\mathbf{x}) - \mathbf{x}\|^2 &= \sum_{j=1}^d \left(\frac{k}{d} ([\mathbf{x}]_j - [\mathbf{x}]_j)^2 + \left(1 - \frac{k}{d}\right) [\mathbf{x}]_j^2 \right) \\ &= \left(1 - \frac{k}{d}\right) \|\mathbf{x}\|^2, \end{aligned}$$

and

$$\begin{aligned}
\mathbb{E}_\omega \left\| \frac{d}{k} \text{rand}_k(\mathbf{x}) - \mathbf{x} \right\|^2 &= \sum_{j=1}^d \left(\frac{k}{d} \left(\frac{d}{k} [\mathbf{x}]_j - [\mathbf{x}]_j \right)^2 + \left(1 - \frac{k}{d} \right) [\mathbf{x}]_j^2 \right) \\
&= \left(\frac{k}{d} \left(\frac{d}{k} - 1 \right)^2 + \left(1 - \frac{k}{d} \right) \right) \sum_{j=1}^d [\mathbf{x}]_j^2 \\
&= \left(\frac{d}{k} - 1 \right) \|\mathbf{x}\|^2,
\end{aligned}$$

For the top_k sparsifier, as $\mathbb{E} \|\text{top}_k(\mathbf{x}) - \mathbf{x}\|^2 \leq \mathbb{E} \|\text{rand}_k(\mathbf{x}) - \mathbf{x}\|^2$, we have

$$\mathbb{E} \|\text{top}_k(\mathbf{x}) - \mathbf{x}\|^2 \leq \left(1 - \frac{k}{d} \right) \|\mathbf{x}\|^2.$$

□

Lemma 10 (Bounded Local Divergence). *The local model difference at round t is bounded as follows:*

$$\frac{1}{n} \sum_{i=1}^n \mathbb{E}_t \|\boldsymbol{\theta}^t - \boldsymbol{\theta}_i^{t,s}\|^2 \leq 32\eta_l^2 \tau^2 \beta^2 \|\nabla f(\boldsymbol{\theta}^t)\|^2 + 32\eta_l^2 \tau^2 \kappa^2 + 4\tau\eta_l^2 \bar{\zeta}^2. \quad (14)$$

where $\bar{\zeta}^2 := (1/n) \sum_{i=1}^n \zeta_i^2$.

Proof. Plugging into the local update rule, we have

$$\begin{aligned}
\mathbb{E}_t \|\boldsymbol{\theta}^t - \boldsymbol{\theta}_i^{t,s}\|^2 &= \mathbb{E}_t \left\| \boldsymbol{\theta}_i^{t,s-1} - \boldsymbol{\theta}^t - \eta_l \mathbf{g}_i^{t,s-1} \right\|^2 \\
&= \mathbb{E}_t \left\| \boldsymbol{\theta}_i^{t,s-1} - \boldsymbol{\theta}^t - \eta_l \mathbf{g}_i^{t,s-1} + \eta_l \nabla f_i(\boldsymbol{\theta}_i^{t,s-1}) - \eta_l \nabla f_i(\boldsymbol{\theta}_i^{t,s-1}) + \eta_l \nabla f_i(\boldsymbol{\theta}^t) - \eta_l \nabla f_i(\boldsymbol{\theta}^t) \right\|^2 \\
&= \mathbb{E}_t \left\| \boldsymbol{\theta}_i^{t,s-1} - \boldsymbol{\theta}^t - \eta_l \nabla f_i(\boldsymbol{\theta}_i^{t,s-1}) + \eta_l \nabla f_i(\boldsymbol{\theta}^t) - \eta_l \nabla f_i(\boldsymbol{\theta}^t) \right\|^2 + \eta_l^2 \mathbb{E}_t \left\| \mathbf{g}_i^{t,s-1} - \nabla f_i(\boldsymbol{\theta}_i^{t,s-1}) \right\|^2 \\
&\leq \left(1 + \frac{1}{2\tau - 1} \right) \mathbb{E}_t \left\| \boldsymbol{\theta}_i^{t,s-1} - \boldsymbol{\theta}^t \right\|^2 + 2\eta_l^2 \tau \mathbb{E}_t \left\| \nabla f_i(\boldsymbol{\theta}_i^{t,s-1}) + \nabla f_i(\boldsymbol{\theta}^t) - \nabla f_i(\boldsymbol{\theta}^t) \right\|^2 + \eta_l^2 \zeta_i^2 \\
&\leq \left(1 + \frac{1}{2\tau - 1} \right) \mathbb{E}_t \left\| \boldsymbol{\theta}_i^{t,s-1} - \boldsymbol{\theta}^t \right\|^2 + 4\eta_l^2 \tau \mathbb{E}_t \left\| \nabla f_i(\boldsymbol{\theta}_i^{t,s-1}) - \nabla f_i(\boldsymbol{\theta}^t) \right\|^2 + 4\eta_l^2 \tau \|\nabla f_i(\boldsymbol{\theta}^t)\|^2 + \eta_l^2 \zeta_i^2 \\
&\leq \left(1 + \frac{1}{2\tau - 1} \right) \mathbb{E}_t \left\| \boldsymbol{\theta}_i^{t,s-1} - \boldsymbol{\theta}^t \right\|^2 + 4\eta_l^2 L^2 \tau \mathbb{E}_t \left\| \boldsymbol{\theta}_i^{t,s-1} - \boldsymbol{\theta}^t \right\|^2 + 4\eta_l^2 \tau \|\nabla f_i(\boldsymbol{\theta}^t)\|^2 + \eta_l^2 \zeta_i^2,
\end{aligned}$$

by using Lemma 6 and Assumption 2, and hence,

$$\begin{aligned}
\frac{1}{n} \sum_{i=1}^n \mathbb{E}_t \|\boldsymbol{\theta}^t - \boldsymbol{\theta}_i^{t,s}\|^2 &\leq \left(1 + \frac{1}{2\tau - 1} + 4\eta_l^2 L^2 \tau \right) \frac{1}{n} \sum_{i=1}^n \mathbb{E}_t \left\| \boldsymbol{\theta}_i^{t,s-1} - \boldsymbol{\theta}^t \right\|^2 + \frac{4\eta_l^2 \tau}{n} \sum_{i=1}^n \mathbb{E}_t \|\nabla f_i(\boldsymbol{\theta}^t)\|^2 + \frac{\eta_l^2}{n} \sum_{i=1}^n \zeta_i^2 \\
&\leq \left(1 + \frac{1}{2\tau - 1} + 4\eta_l^2 L^2 \tau \right) \frac{1}{n} \sum_{i=1}^n \mathbb{E}_t \left\| \boldsymbol{\theta}_i^{t,s-1} - \boldsymbol{\theta}^t \right\|^2 + 8\eta_l^2 \tau \beta^2 \|\nabla f(\boldsymbol{\theta}^t)\|^2 + 8\eta_l^2 \tau \kappa^2 + \frac{\eta_l^2}{n} \sum_{i=1}^n \zeta_i^2 \\
&\leq \left(1 + \frac{1}{\tau - 1} \right) \frac{1}{n} \sum_{i=1}^n \mathbb{E}_t \left\| \boldsymbol{\theta}_i^{t,s-1} - \boldsymbol{\theta}^t \right\|^2 + 8\eta_l^2 \tau \beta^2 \|\nabla f(\boldsymbol{\theta}^t)\|^2 + 8\eta_l^2 \tau \kappa^2 + \frac{\eta_l^2}{n} \sum_{i=1}^n \zeta_i^2, \quad (15)
\end{aligned}$$

when $\eta_l \leq 1/3\tau L$. Unrolling the recursion, we obtain the following:

$$\begin{aligned}
\frac{1}{n} \sum_{i=1}^n \mathbb{E}_t \|\boldsymbol{\theta}^t - \boldsymbol{\theta}_i^s\|^2 &\leq \sum_{h=0}^{s-1} \left(1 + \frac{1}{\tau - 1} \right)^h \left[8\eta_l^2 \tau \beta^2 \|\nabla f(\boldsymbol{\theta}^t)\|^2 + 8\eta_l^2 \tau \kappa^2 + \frac{\eta_l^2}{n} \sum_{i=1}^n \zeta_i^2 \right] \\
&\leq (\tau - 1) \left[\left(1 + \frac{1}{\tau - 1} \right)^\tau - 1 \right] \times \left[8\eta_l^2 \tau \beta^2 \|\nabla f(\boldsymbol{\theta}^t)\|^2 + 8\eta_l^2 \tau \kappa^2 + \frac{\eta_l^2}{n} \sum_{i=1}^n \zeta_i^2 \right] \\
&\leq 32\eta_l^2 \tau^2 \beta^2 \|\nabla f(\boldsymbol{\theta}^t)\|^2 + 32\eta_l^2 \tau^2 \kappa^2 + \frac{4\tau\eta_l^2}{n} \sum_{i=1}^n \zeta_i^2, \quad (16)
\end{aligned}$$

where the last inequality results from the fact that $\left(1 + \frac{1}{\tau - 1} \right)^\tau \leq 5$ when $\tau > 1$. □

Lemma 11 (Bounded Local Model Update). *The local model update \mathbf{d}_i^t at round t is bounded as follows:*

$$\frac{1}{n} \sum_{i=1}^n \mathbb{E}_t \|\mathbf{d}_i^t\|^2 \leq \frac{L^2}{n\tau} \sum_{i=1}^n \sum_{s=0}^{\tau-1} \mathbb{E}_t \|\boldsymbol{\theta}^t - \boldsymbol{\theta}_i^{t,s}\|^2 + 2(\beta^2 \|\nabla f(\boldsymbol{\theta}^t)\|^2 + \kappa^2) + \bar{\zeta}^2. \quad (17)$$

where $\bar{\zeta}^2 := (1/n) \sum_{i=1}^n \zeta_i^2$.

Proof. Since $\mathbb{E}_t[\mathbf{d}_i^t] = \mathbf{h}_i^t$, we have

$$\begin{aligned} \frac{1}{n} \sum_{i=1}^n \mathbb{E}_t \|\mathbf{d}_i^t\|^2 &= \frac{1}{n} \sum_{i=1}^n \mathbb{E}_t \|\mathbf{d}_i^t - \mathbf{h}_i^t + \mathbf{h}_i^t\|^2 \\ &= \frac{1}{n} \sum_{i=1}^n \left[\mathbb{E}_t \|\mathbf{d}_i^t - \mathbf{h}_i^t\|^2 + \mathbb{E}_t \|\mathbf{h}_i^t\|^2 + \mathbb{E}_t \langle \mathbf{d}_i^t - \mathbf{h}_i^t, \mathbf{h}_i^t \rangle \right] \\ &= \frac{1}{n} \sum_{i=1}^n \left[\mathbb{E}_t \|\mathbf{d}_i^t - \mathbf{h}_i^t\|^2 + \mathbb{E}_t \|\mathbf{h}_i^t\|^2 \right] \\ &= \frac{1}{n} \sum_{i=1}^n \left[\mathbb{E}_t \|\mathbf{d}_i^t - \mathbf{h}_i^t\|^2 + \mathbb{E}_t \|\mathbf{h}_i^t - \nabla f_i(\boldsymbol{\theta}^t) + \nabla f_i(\boldsymbol{\theta}^t)\|^2 \right] \\ &\leq \frac{1}{n} \sum_{i=1}^n \left[\mathbb{E}_t \|\mathbf{d}_i^t - \mathbf{h}_i^t\|^2 + 2\mathbb{E}_t \|\mathbf{h}_i^t - \nabla f_i(\boldsymbol{\theta}^t)\|^2 \right] + \frac{2}{n} \sum_{i=1}^n \mathbb{E}_t \|\nabla f_i(\boldsymbol{\theta}^t)\|^2 \\ &\leq \frac{1}{n} \sum_{i=1}^n \left[\mathbb{E}_t \|\mathbf{d}_i^t - \mathbf{h}_i^t\|^2 + 2\mathbb{E}_t \|\mathbf{h}_i^t - \nabla f_i(\boldsymbol{\theta}^t)\|^2 \right] + 2(\beta^2 \|\nabla f(\boldsymbol{\theta}^t)\|^2 + \kappa^2) \end{aligned} \quad (18)$$

where the first inequality uses Lemma 6, and the last inequality uses Assumption 3. Given that

$$\mathbb{E}_t \|\mathbf{d}_i^t - \mathbf{h}_i^t\|^2 = \mathbb{E}_t \left\| \frac{1}{\tau} \sum_{s=0}^{\tau-1} (\mathbf{g}_i^{t,s} - \nabla f_i(\boldsymbol{\theta}_i^{t,s})) \right\|^2 \leq \frac{1}{\tau} \sum_{s=0}^{\tau-1} \mathbb{E}_t \|\mathbf{g}_i^{t,s} - \nabla f_i(\boldsymbol{\theta}_i^{t,s})\|^2 \leq \frac{1}{\tau} \sum_{s=0}^{\tau-1} \zeta_i^2 = \zeta_i^2, \quad (19)$$

by Lemma 6 and Assumption 2, and

$$\mathbb{E}_t \|\mathbf{h}_i^t - \nabla f_i(\boldsymbol{\theta}^t)\|^2 = \mathbb{E}_t \left\| \frac{1}{\tau} \sum_{s=0}^{\tau-1} (\nabla f_i(\boldsymbol{\theta}_i^{t,s}) - \nabla f_i(\boldsymbol{\theta}^t)) \right\|^2 \leq \frac{1}{\tau} \sum_{s=0}^{\tau-1} \mathbb{E}_t \|\nabla f_i(\boldsymbol{\theta}_i^{t,s}) - \nabla f_i(\boldsymbol{\theta}^t)\|^2 \leq \frac{L^2}{\tau} \sum_{s=0}^{\tau-1} \mathbb{E}_t \|\boldsymbol{\theta}^t - \boldsymbol{\theta}_i^{t,s}\|^2 \quad (20)$$

by Lemma 6 and the L -smoothness of function f_i , one yields

$$\frac{1}{n} \sum_{i=1}^n \mathbb{E}_t \|\mathbf{d}_i^t\|^2 \leq \bar{\zeta}^2 + \frac{1}{n} \sum_{i=1}^n \frac{L^2}{\tau} \sum_{s=0}^{\tau-1} \mathbb{E}_t \|\boldsymbol{\theta}^t - \boldsymbol{\theta}_i^{t,s}\|^2 + 2(\beta^2 \|\nabla f(\boldsymbol{\theta}^t)\|^2 + \kappa^2). \quad (21)$$

□

D. Proof of Theorem 1

Suppose the client is sampled without replacement with probability $q = r/n$ at each round. By Lemma 2 and Lemma 3, the t -th round of Fed-SMP satisfies $(\alpha, \rho_t(\alpha))$ -RDP, where

$$\rho_t(\alpha) = \frac{3.5q^2\alpha}{\sigma^2}, \quad (22)$$

if $\sigma^2 \geq 0.7$ and $\alpha \leq 1 + (2/3)C^2\sigma^2 \log(1/q\alpha(1 + \sigma^2))$. Then by Lemma 4, Fed-SMP satisfies $(\alpha, T\rho_t(\alpha))$ -RDP after T rounds of training. Next, in order to guarantee (ϵ, δ) -DP according to Lemma 1, we need

$$\frac{3.5q^2T\alpha}{\sigma^2} + \frac{\log(1/\delta)}{\alpha - 1} \leq \epsilon. \quad (23)$$

Suppose α and σ are chosen such that the conditions for (22) are satisfied. Choose $\alpha = 1 + 2\log(1/\delta)/\epsilon$ and rearrange the inequality in (23), we need

$$\sigma^2 \geq \frac{7q^2T(\epsilon + 2\log(1/\delta))}{\epsilon^2}. \quad (24)$$

Then using the constraint on ϵ concludes the proof.

E. Proof of Theorem 2 with rand_k sparsifier

Let $\text{spar} := (d/k) \text{rand}_k$ denote the unbiased random sparsifier. By the L -smoothness of function f , we have

$$\begin{aligned}
\mathbb{E}_t[f(\boldsymbol{\theta}^{t+1}) - f(\boldsymbol{\theta}^t)] &\leq \mathbb{E}_t \langle \nabla f(\boldsymbol{\theta}^t), \boldsymbol{\theta}^{t+1} - \boldsymbol{\theta}^t \rangle + \frac{L}{2} \mathbb{E}_t \|\boldsymbol{\theta}^{t+1} - \boldsymbol{\theta}^t\|^2 \\
&= -\mathbb{E}_t \left\langle \nabla f(\boldsymbol{\theta}^t), \mathbb{E}_{\mathcal{W}^t} \left[\frac{1}{r} \sum_{i \in \mathcal{W}^t} \Delta_i^t \right] \right\rangle + \frac{L}{2} \mathbb{E}_t \left\| \frac{1}{r} \sum_{i \in \mathcal{W}^t} \Delta_i^t \right\|^2 \\
&= -\mathbb{E}_t \left\langle \nabla f(\boldsymbol{\theta}^t), \frac{1}{n} \sum_{i=1}^n \Delta_i^t \right\rangle + \frac{L}{2} \mathbb{E}_t \left\| \frac{1}{r} \sum_{i \in \mathcal{W}^t} \Delta_i^t \right\|^2 \\
&= \underbrace{-\mathbb{E}_t \left\langle \nabla f(\boldsymbol{\theta}^t), \frac{1}{n} \sum_{i=1}^n (\eta_l \tau \text{spar}(\mathbf{d}_i^t) + \mathbf{b}_i^t) \right\rangle}_{T_1} + \underbrace{\frac{L}{2} \mathbb{E}_t \left\| \frac{1}{r} \sum_{i \in \mathcal{W}^t} (\eta_l \tau \text{spar}(\mathbf{d}_i^t) + \mathbf{b}_i^t) \right\|^2}_{T_2} \tag{25}
\end{aligned}$$

where the expectation $\mathbb{E}_t[\cdot]$ is taken over the sampled clients \mathcal{W}^t and mini-batches $\xi_i^s, \forall i \in [n], s \in \{0, \dots, \tau - 1\}$ at round t and the sparsifier spar . As $\text{spar} = (d/k) \text{rand}_k$, due to the unbiasedness of the stochastic gradient and Gaussian noise, we have

$$\begin{aligned}
T_1 &= -\left\langle \nabla f(\boldsymbol{\theta}^t), \mathbb{E}_t \left[\frac{1}{n} \sum_{i=1}^n \eta_l \tau \mathbf{d}_i^t \right] \right\rangle - \left\langle \nabla f(\boldsymbol{\theta}^t), \mathbb{E}_t \left[\frac{1}{n} \sum_{i=1}^n \mathbf{b}_i^t \right] \right\rangle \\
&= -\eta_l \tau \mathbb{E}_t \left\langle \nabla f(\boldsymbol{\theta}^t), \frac{1}{n} \sum_{i=1}^n \mathbf{h}_i^t \right\rangle \\
&= -\frac{\eta_l \tau}{2} \|\nabla f(\boldsymbol{\theta}^t)\|^2 - \frac{\eta_l \tau}{2} \mathbb{E}_t \left\| \frac{1}{n} \sum_{i=1}^n \mathbf{h}_i^t \right\|^2 + \frac{\eta_l \tau}{2} \mathbb{E}_t \left\| \nabla f(\boldsymbol{\theta}^t) - \frac{1}{n} \sum_{i=1}^n \mathbf{h}_i^t \right\|^2 \\
&\leq -\frac{\eta_l \tau}{2} \|\nabla f(\boldsymbol{\theta}^t)\|^2 + \frac{\eta_l \tau}{2} \mathbb{E}_t \left\| \frac{1}{n} \sum_{i=1}^n \frac{1}{\tau} \sum_{s=0}^{\tau-1} (\nabla f_i(\boldsymbol{\theta}^t) - \nabla f_i(\boldsymbol{\theta}_i^{t,s})) \right\|^2 \\
&\leq -\frac{\eta_l \tau}{2} \|\nabla f(\boldsymbol{\theta}^t)\|^2 + \frac{\eta_l \tau}{2n} \sum_{i=1}^n \frac{1}{\tau} \sum_{s=0}^{\tau-1} \mathbb{E}_t \|\nabla f_i(\boldsymbol{\theta}^t) - \nabla f_i(\boldsymbol{\theta}_i^{t,s})\|^2 \\
&\leq -\frac{\eta_l \tau}{2} \|\nabla f(\boldsymbol{\theta}^t)\|^2 + \frac{\eta_l L^2}{2n} \sum_{i=1}^n \sum_{s=0}^{\tau-1} \mathbb{E}_t \|\boldsymbol{\theta}^t - \boldsymbol{\theta}_i^{t,s}\|^2, \tag{26}
\end{aligned}$$

where the first inequality results from the fact that $\|(1/n) \sum_{i=1}^n \mathbf{h}_i^t\|^2 \geq 0$, the second inequality uses Lemma 6, and the third inequality uses the L -smoothness of function f_i .

For T_2 , let $\phi_k := d/k - 1$, we have

$$\begin{aligned}
T_2 &\leq \frac{L\eta_l^2 \tau^2}{2} \mathbb{E}_t \left[\frac{1}{r} \sum_{i \in \mathcal{W}^t} \|\text{spar}(\mathbf{d}_i^t)\|^2 \right] + \frac{L}{2} \mathbb{E}_t \left\| \frac{1}{r} \sum_{i \in \mathcal{W}^t} \mathbf{b}_i^t \right\|^2 \\
&= \frac{L\eta_l^2 \tau^2}{2n} \sum_{i=1}^n \mathbb{E}_t \|\text{spar}(\mathbf{d}_i^t) - \mathbf{d}_i^t + \mathbf{d}_i^t\|^2 + \frac{LkC^2\sigma^2}{2r^2} \\
&\leq \frac{L\eta_l^2 \tau^2}{2n} \sum_{i=1}^n \mathbb{E}_t \left[2\|\text{spar}(\mathbf{d}_i^t) - \mathbf{d}_i^t\|^2 + 2\|\mathbf{d}_i^t\|^2 \right] + \frac{LC^2k\sigma^2}{2r^2} \\
&\leq \frac{L\eta_l^2 \tau^2 (\phi_k + 1)}{n} \sum_{i=1}^n \mathbb{E}_t \|\mathbf{d}_i^t\|^2 + \frac{LC^2k\sigma^2}{2r^2} \tag{27}
\end{aligned}$$

where the first inequality uses the independence of Gaussian noise and Lemma 6, the second inequality also uses Lemma 6, and the last inequality results from Lemma 9. By Lemma 11, T_2 is bounded as follows:

$$T_2 \leq 2L\eta_l^2 \tau^2 (\phi_k + 1) \beta^2 \|\nabla f(\boldsymbol{\theta}^t)\|^2 + \frac{L^3 \eta_l^2 \tau (\phi_k + 1)}{n} \sum_{i=1}^n \sum_{s=0}^{\tau-1} \mathbb{E}_t \|\boldsymbol{\theta}^t - \boldsymbol{\theta}_i^{t,s}\|^2 + L\eta_l^2 \tau^2 (\phi_k + 1) (\bar{\zeta}^2 + 2\kappa^2) + \frac{LC^2k\sigma^2}{2r^2} \tag{28}$$

Combining (25), (26) and (28), one yields

$$\begin{aligned}
\mathbb{E}_t[f(\boldsymbol{\theta}^{t+1}) - f(\boldsymbol{\theta}^t)] &\leq \left(-\frac{\eta\tau}{2} + 2L\eta_l^2\tau^2(\phi_k + 1)\beta^2\right) \|\nabla f(\boldsymbol{\theta}^t)\|^2 \\
&\quad + \frac{\eta_l L^2 + 2L^3\eta_l^2\tau(\phi_k + 1)}{2n} \sum_{i=1}^n \sum_{s=0}^{\tau-1} \mathbb{E}_t \|\boldsymbol{\theta}^t - \boldsymbol{\theta}_i^{t,s}\|^2 + L\eta_l^2\tau^2(\phi_k + 1)(\bar{\zeta}^2 + 2\kappa^2) + \frac{LC^2k\sigma^2}{2r^2} \\
&\leq -\frac{\eta\tau}{4} \|\nabla f(\boldsymbol{\theta}^t)\|^2 + \frac{\eta_l L^2(4\beta^2 + 1)}{8n\beta^2} \sum_{i=1}^n \sum_{s=0}^{\tau-1} \mathbb{E}_t \|\boldsymbol{\theta}^t - \boldsymbol{\theta}_i^{t,s}\|^2 + L\eta_l^2\tau^2(\phi_k + 1)(\bar{\zeta}^2 + 2\kappa^2) + \frac{LkC^2\sigma^2}{2r^2},
\end{aligned} \tag{29}$$

if we choose $\eta_l \leq 1/8\tau L(\phi_k + 1)\beta^2$. Next, by Lemma 10, we obtain that

$$\begin{aligned}
\mathbb{E}_t[f(\boldsymbol{\theta}^{t+1}) - f(\boldsymbol{\theta}^t)] &\leq -\frac{\eta\tau}{4} \|\nabla f(\boldsymbol{\theta}^t)\|^2 + \frac{\eta_l L^2(4\beta^2 + 1)}{8\beta^2} \sum_{s=0}^{\tau-1} \left[32\eta_l^2\tau^2\beta^2 \|\nabla f(\boldsymbol{\theta}^t)\|^2 + 32\eta_l^2\tau^2\kappa^2 + 4\tau\eta_l^2\bar{\zeta}^2\right] \\
&\quad + L\eta_l^2\tau^2(\phi_k + 1)(\bar{\zeta}^2 + 2\kappa^2) + \frac{LC^2k\sigma^2}{2r^2} \\
&= \left(-\frac{\eta\tau}{4} + 4\eta_l L^2(4\beta^2 + 1)\eta_l^2\tau^3\right) \|\nabla f(\boldsymbol{\theta}^t)\|^2 + \frac{\eta_l^3\tau^2 L^2(4\beta^2 + 1)(8\tau\kappa^2 + \bar{\zeta}^2)}{2\beta^2} \\
&\quad + L\eta_l^2\tau^2(\phi_k + 1)(\bar{\zeta}^2 + 2\kappa^2) + \frac{LC^2k\sigma^2}{2r^2} \\
&\leq -\frac{\eta\tau}{8} \|\nabla f(\boldsymbol{\theta}^t)\|^2 + \eta_l^2\tau^2 L(24\tau\eta_l L + 2)\kappa^2 + \eta_l^2\tau^2 L(3\eta_l L + 1)\bar{\zeta}^2 \\
&\quad + L\eta_l^2\tau^2\phi_k(\bar{\zeta}^2 + 2\kappa^2) + \frac{LC^2k\sigma^2}{2r^2} \\
&\leq -\frac{\eta\tau}{8} \|\nabla f(\boldsymbol{\theta}^t)\|^2 + \eta_l^2\tau^2 L(3\kappa^2 + 2\bar{\zeta}^2) + \eta_l^2\tau^2 L(2\kappa^2 + \bar{\zeta}^2)\phi_k + \frac{LC^2k\sigma^2}{2r^2}
\end{aligned} \tag{30}$$

if $\eta_l \leq \min\{1/16\tau L\sqrt{8\beta^2 + 2}, 1/24\tau L\}$. Rearranging the above inequality in (30) and summing it from $t = 0$ to $T - 1$, we get

$$\begin{aligned}
\sum_{t=0}^{T-1} \|\nabla f(\boldsymbol{\theta}^t)\|^2 &\leq \frac{8}{\eta\tau} \mathbb{E}\left[\sum_{t=0}^{T-1} f(\boldsymbol{\theta}^t) - f(\boldsymbol{\theta}^{t+1})\right] + 8T\eta_l\tau L(3\kappa^2 + 2\bar{\zeta}^2) + 8T\eta_l\tau L(2\kappa^2 + \bar{\zeta}^2)\phi_k + \frac{4TLC^2k\sigma^2}{\eta_l\tau r^2} \\
&\leq \frac{8(f(\boldsymbol{\theta}^0) - f(\boldsymbol{\theta}^*))}{\eta\tau} + 8T\eta_l\tau L(3\kappa^2 + 2\bar{\zeta}^2) + 8T\eta_l\tau L(2\kappa^2 + \bar{\zeta}^2)\phi_k + \frac{4TLC^2k\sigma^2}{\eta_l\tau r^2},
\end{aligned} \tag{31}$$

where the expectation is taken over all rounds $t \in [0, T - 1]$. Dividing both sides of (31) by T , one yields

$$\frac{1}{T} \sum_{t=0}^{T-1} \|\nabla f(\boldsymbol{\theta}^t)\|^2 \leq \frac{8(f(\boldsymbol{\theta}^0) - f^*)}{T\eta\tau} + 8\eta_l\tau L(3\kappa^2 + 2\bar{\zeta}^2) + 8\eta_l\tau L(2\kappa^2 + \bar{\zeta}^2)\phi_k + \frac{4LC^2k\sigma^2}{\eta_l\tau r^2},$$

if the learning rates η_l satisfy $\eta_l \leq \min\{1/8\tau L(\phi_k + 1)\beta^2, 1/16\tau L\sqrt{8\beta^2 + 2}, 1/24\tau L\}$. Here, we use the fact that $f^* \leq f(\boldsymbol{\theta}^T)$.

F. Proof of Theorem 2 with top_k sparsifier

Here, spar represents the operation of top_k sparsification in Fed-SMP, and we assume that the distribution of the public distribution is similar to the overall distribution $\{\mathcal{D}_i\}_{i \in [n]}$. By the L -smoothness of function f , we have

$$\begin{aligned}
\mathbb{E}_t[f(\boldsymbol{\theta}^{t+1}) - f(\boldsymbol{\theta}^t)] &\leq \mathbb{E}_t \langle \nabla f(\boldsymbol{\theta}^t), \boldsymbol{\theta}^{t+1} - \boldsymbol{\theta}^t \rangle + \frac{L}{2} \mathbb{E}_t \|\boldsymbol{\theta}^{t+1} - \boldsymbol{\theta}^t\|^2 \\
&= -\mathbb{E}_t \left\langle \nabla f(\boldsymbol{\theta}^t), \mathbb{E}_{\mathcal{W}^t} \left[\frac{1}{r} \sum_{i \in \mathcal{W}^t} \Delta_i^t \right] \right\rangle + \frac{L}{2} \mathbb{E}_t \left\| \frac{1}{r} \sum_{i \in \mathcal{W}^t} \Delta_i^t \right\|^2 \\
&= -\mathbb{E}_t \left\langle \nabla f(\boldsymbol{\theta}^t), \frac{1}{n} \sum_{i=1}^n \Delta_i^t \right\rangle + \frac{L}{2} \mathbb{E}_t \left\| \frac{1}{r} \sum_{i \in \mathcal{W}^t} \Delta_i^t \right\|^2 \\
&= \underbrace{-\mathbb{E}_t \left\langle \nabla f(\boldsymbol{\theta}^t), \frac{1}{n} \sum_{i=1}^n (\eta_l \tau \text{spar}(\mathbf{d}_i^t) + \mathbf{b}_i^t) \right\rangle}_{T_1} + \underbrace{\frac{L}{2} \mathbb{E}_t \left\| \frac{1}{r} \sum_{i \in \mathcal{W}^t} (\eta_l \tau \text{spar}(\mathbf{d}_i^t) + \mathbf{b}_i^t) \right\|^2}_{T_2} \quad (32)
\end{aligned}$$

where the expectation $\mathbb{E}_t[\cdot]$ is taken over the sampled clients \mathcal{W}^t and mini-batches $\xi_i^s, \forall i \in [n], s \in \{0, \dots, \tau - 1\}$ at round t . Due to the unbiasedness of the stochastic gradient and Gaussian noise, we have

$$\begin{aligned}
T_1 &= -\left\langle \nabla f(\boldsymbol{\theta}^t), \mathbb{E}_t \left[\frac{1}{n} \sum_{i=1}^n \eta_l \tau \mathbf{d}_i^t \right] \right\rangle + \left\langle \nabla f(\boldsymbol{\theta}^t), \mathbb{E}_t \left[\frac{1}{n} \sum_{i=1}^n \eta_l \tau \mathbf{d}_i^t - \frac{1}{n} \sum_{i=1}^n \eta_l \tau \text{spar}(\mathbf{d}_i^t) \right] \right\rangle - \left\langle \nabla f(\boldsymbol{\theta}^t), \mathbb{E}_t \left[\frac{1}{n} \sum_{i=1}^n \mathbf{b}_i^t \right] \right\rangle \\
&= \underbrace{-\eta_l \tau \mathbb{E}_t \left\langle \nabla f(\boldsymbol{\theta}^t), \frac{1}{n} \sum_{i=1}^n \mathbf{h}_i^t \right\rangle}_{A_1} + \underbrace{\eta_l \tau \left\langle \nabla f(\boldsymbol{\theta}^t), \mathbb{E}_t \left[\frac{1}{n} \sum_{i=1}^n \mathbf{d}_i^t - \text{spar} \left(\frac{1}{n} \sum_{i=1}^n \mathbf{d}_i^t \right) \right] \right\rangle}_{A_2} \quad (33)
\end{aligned}$$

since the clients at each round use the same top_k sparsifier. Using the fact that $2\langle a, b \rangle = \|a\|^2 + \|b\|^2 - \|a - b\|^2$, we have

$$\begin{aligned}
A_1 &= -\frac{\eta_l \tau}{2} \|\nabla f(\boldsymbol{\theta}^t)\|^2 - \frac{\eta_l \tau}{2} \mathbb{E}_t \left\| \frac{1}{n} \sum_{i=1}^n \mathbf{h}_i^t \right\|^2 + \frac{\eta_l \tau}{2} \mathbb{E}_t \left\| \nabla f(\boldsymbol{\theta}^t) - \frac{1}{n} \sum_{i=1}^n \mathbf{h}_i^t \right\|^2 \\
&= -\frac{\eta_l \tau}{2} \|\nabla f(\boldsymbol{\theta}^t)\|^2 + \frac{\eta_l \tau}{2} \mathbb{E}_t \left\| \frac{1}{n} \sum_{i=1}^n \frac{1}{\tau} \sum_{s=0}^{\tau-1} (\nabla f_i(\boldsymbol{\theta}^t) - \nabla f_i(\boldsymbol{\theta}_i^{t,s})) \right\|^2 - \frac{\eta_l \tau}{2} \mathbb{E}_t \left\| \frac{1}{n} \sum_{i=1}^n \mathbf{h}_i^t \right\|^2 \\
&\leq -\frac{\eta_l \tau}{2} \|\nabla f(\boldsymbol{\theta}^t)\|^2 + \frac{\eta_l \tau}{2n} \sum_{i=1}^n \frac{1}{\tau} \sum_{s=0}^{\tau-1} \mathbb{E}_t \|\nabla f_i(\boldsymbol{\theta}^t) - \nabla f_i(\boldsymbol{\theta}_i^{t,s})\|^2 - \frac{\eta_l \tau}{2} \mathbb{E}_t \left\| \frac{1}{n} \sum_{i=1}^n \mathbf{h}_i^t \right\|^2 \\
&\leq -\frac{\eta_l \tau}{2} \|\nabla f(\boldsymbol{\theta}^t)\|^2 + \frac{\eta_l L^2}{2n} \sum_{i=1}^n \sum_{s=0}^{\tau-1} \mathbb{E}_t \|\boldsymbol{\theta}^t - \boldsymbol{\theta}_i^{t,s}\|^2 - \frac{\eta_l \tau}{2} \mathbb{E}_t \left\| \frac{1}{n} \sum_{i=1}^n \mathbf{h}_i^t \right\|^2, \quad (34)
\end{aligned}$$

where the first inequality uses Lemma 6, and the second inequality uses the L -smoothness of function f_i . Next, let $\phi_k := 1 - k/d$, we get

$$\begin{aligned}
A_2 &\leq \frac{\eta\tau}{2} \left(\gamma \|\nabla f(\boldsymbol{\theta}^t)\|^2 + \gamma^{-1} \mathbb{E}_t \left\| \frac{1}{n} \sum_{i=1}^n \mathbf{d}_i^t - \text{spar} \left(\frac{1}{n} \sum_{i=1}^n \mathbf{d}_i^t \right) \right\|^2 \right) \\
&\leq \frac{\eta\tau\gamma}{2} \|\nabla f(\boldsymbol{\theta}^t)\|^2 + \frac{\eta\tau\phi_k}{2\gamma} \mathbb{E}_t \left\| \frac{1}{n} \sum_{i=1}^n \mathbf{d}_i^t \right\|^2 \\
&= \frac{\eta\tau\gamma}{2} \|\nabla f(\boldsymbol{\theta}^t)\|^2 + \frac{\eta\tau\phi_k}{2\gamma} \mathbb{E}_t \left\| \frac{1}{n} \sum_{i=1}^n \mathbf{d}_i^t - \frac{1}{n} \sum_{i=1}^n \mathbf{h}_i^t + \frac{1}{n} \sum_{i=1}^n \mathbf{h}_i^t \right\|^2 \\
&= \frac{\eta\tau\gamma}{2} \|\nabla f(\boldsymbol{\theta}^t)\|^2 + \frac{\eta\tau\phi_k}{2\gamma} \mathbb{E}_t \left[\left\| \frac{1}{n} \sum_{i=1}^n \mathbf{d}_i^t - \frac{1}{n} \sum_{i=1}^n \mathbf{h}_i^t \right\|^2 + \left\| \frac{1}{n} \sum_{i=1}^n \mathbf{h}_i^t \right\|^2 + 2 \left\langle \frac{1}{n} \sum_{i=1}^n \mathbf{h}_i^t, \frac{1}{n} \sum_{i=1}^n \mathbf{d}_i^t - \frac{1}{n} \sum_{i=1}^n \mathbf{h}_i^t \right\rangle \right] \\
&= \frac{\eta\tau\gamma}{2} \|\nabla f(\boldsymbol{\theta}^t)\|^2 + \frac{\eta\tau\phi_k}{2\gamma} \mathbb{E}_t \left[\left\| \frac{1}{n} \sum_{i=1}^n \mathbf{d}_i^t - \frac{1}{n} \sum_{i=1}^n \mathbf{h}_i^t \right\|^2 + \left\| \frac{1}{n} \sum_{i=1}^n \mathbf{h}_i^t \right\|^2 \right] \tag{35}
\end{aligned}$$

$$\leq \frac{\eta\tau\gamma}{2} \|\nabla f(\boldsymbol{\theta}^t)\|^2 + \frac{\eta\tau\phi_k}{2n\gamma} \sum_{i=1}^n \mathbb{E}_t \|\mathbf{d}_i^t - \mathbf{h}_i^t\|^2 + \frac{\eta\tau\phi_k}{2\gamma} \mathbb{E}_t \left\| \frac{1}{n} \sum_{i=1}^n \mathbf{h}_i^t \right\|^2, \tag{36}$$

where the first inequality uses Lemma 13, the second inequality uses Lemma 9, and the third inequality uses Lemma 6. Given that

$$\mathbb{E}_t \|\mathbf{d}_i^t - \mathbf{h}_i^t\|^2 = \mathbb{E}_t \left\| \frac{1}{\tau} \sum_{s=0}^{\tau-1} (\mathbf{g}_i^{t,s} - \nabla f_i(\boldsymbol{\theta}_i^{t,s})) \right\|^2 \leq \frac{1}{\tau} \sum_{s=0}^{\tau-1} \mathbb{E}_t \|\mathbf{g}_i^{t,s} - \nabla f_i(\boldsymbol{\theta}_i^{t,s})\|^2 \leq \frac{1}{\tau} \sum_{s=0}^{\tau-1} \zeta_i^2 = \zeta_i^2, \tag{37}$$

by Lemma 6 and Assumption 2, we have

$$A_2 \leq \frac{\eta\tau\gamma}{2} \|\nabla f(\boldsymbol{\theta}^t)\|^2 + \frac{\eta\tau\phi_k}{2n\gamma} \sum_{i=1}^n \zeta_i^2 + \frac{\eta\tau\phi_k}{2\gamma} \mathbb{E}_t \left\| \frac{1}{n} \sum_{i=1}^n \mathbf{h}_i^t \right\|^2. \tag{38}$$

Combining (33), (34) and (35) and let $\bar{\zeta}^2 := (1/n) \sum_{i=1}^n \zeta_i^2$, we get

$$\begin{aligned}
T_1 &\leq -\frac{\eta\tau(1-\gamma)}{2} \|\nabla f(\boldsymbol{\theta}^t)\|^2 + \frac{\eta\tau L^2}{2n} \sum_{i=1}^n \frac{1}{\tau} \sum_{s=0}^{\tau-1} \mathbb{E}_t \|\boldsymbol{\theta}^t - \boldsymbol{\theta}_i^{t,s}\|^2 - \frac{\eta\tau(1-\phi_k/\gamma)}{2} \mathbb{E}_t \left\| \frac{1}{n} \sum_{i=1}^n \mathbf{h}_i^t \right\|^2 + \frac{\eta\tau\phi_k \bar{\zeta}^2}{2\gamma} \\
&\leq -\frac{\eta\tau(1-\gamma)}{2} \|\nabla f(\boldsymbol{\theta}^t)\|^2 + \frac{\eta\tau L^2}{2n} \sum_{i=1}^n \sum_{s=0}^{\tau-1} \mathbb{E}_t \|\boldsymbol{\theta}^t - \boldsymbol{\theta}_i^{t,s}\|^2 + \frac{\eta\tau\phi_k \bar{\zeta}^2}{2\gamma}, \tag{39}
\end{aligned}$$

if $\phi_k \leq \gamma$.

To bound T_2 , we utilize the independence of Gaussian noise and obtain that

$$\begin{aligned}
T_2 &= \frac{L\eta_l^2\tau^2}{2}\mathbb{E}_t\left\|\text{spar}\left(\frac{1}{r}\sum_{i\in\mathcal{W}^t}\mathbf{d}_i^t\right)\right\|^2 + \frac{L}{2}\mathbb{E}_t\left\|\frac{1}{r}\sum_{i\in\mathcal{W}^t}\mathbf{b}_i^t\right\|^2 \\
&= \frac{L\eta_l^2\tau^2}{2}\mathbb{E}_t\left\|\text{spar}\left(\frac{1}{r}\sum_{i\in\mathcal{W}^t}\mathbf{d}_i^t\right) - \frac{1}{r}\sum_{i\in\mathcal{W}^t}\mathbf{d}_i^t + \frac{1}{r}\sum_{i\in\mathcal{W}^t}\mathbf{d}_i^t\right\|^2 + \frac{LkC^2\sigma^2}{2r^2} \\
&\leq L\eta_l^2\tau^2\mathbb{E}_t\left\|\text{spar}\left(\frac{1}{r}\sum_{i\in\mathcal{W}^t}\mathbf{d}_i^t\right) - \frac{1}{r}\sum_{i\in\mathcal{W}^t}\mathbf{d}_i^t\right\|^2 + L\eta_l^2\tau^2\mathbb{E}_t\left\|\frac{1}{r}\sum_{i\in\mathcal{W}^t}\mathbf{d}_i^t\right\|^2 + \frac{LkC^2\sigma^2}{2r^2} \\
&\leq L\eta_l^2\tau^2(\phi_k+1)\mathbb{E}_t\left\|\frac{1}{r}\sum_{i\in\mathcal{W}^t}\mathbf{d}_i^t\right\|^2 + \frac{LkC^2\sigma^2}{2r^2} \\
&\leq L\eta_l^2\tau^2(\phi_k+1)\mathbb{E}_t\left[\frac{1}{r}\sum_{i\in\mathcal{W}^t}\|\mathbf{d}_i^t\|^2\right] + \frac{LkC^2\sigma^2}{2r^2} \\
&= L\eta_l^2\tau^2(\phi_k+1)\mathbb{E}_t\left[\frac{1}{n}\sum_{i=1}^n\|\mathbf{d}_i^t\|^2\right] + \frac{LkC^2\sigma^2}{2r^2}, \tag{40}
\end{aligned}$$

where the first inequality uses the fact that $\|a+b\|^2 \leq 2\|a\|^2 + 2\|b\|^2$, the second inequality uses Lemma 9, and the last inequality results from Lemma 6. Then, by Lemma 11, we get

$$T_2 \leq L\eta_l^2\tau^2(\phi_k+1)\left(\frac{L^2}{n\tau}\sum_{i=1}^n\sum_{s=0}^{\tau-1}\mathbb{E}_t\|\boldsymbol{\theta}^t - \boldsymbol{\theta}_{i,s}^{t,s}\|^2 + 2(\beta^2\|\nabla f(\boldsymbol{\theta}^t)\|^2 + \kappa^2) + \bar{\zeta}^2\right) + \frac{LkC^2\sigma^2}{2r^2} \tag{41}$$

Combining (32), (39) and (41), one yields

$$\begin{aligned}
\mathbb{E}_t[f(\boldsymbol{\theta}^{t+1}) - f(\boldsymbol{\theta}^t)] &\leq \left(-\frac{\eta_l\tau(1-\gamma)}{2} + 2L\eta_l^2\tau^2(\phi_k+1)\beta^2\right)\|\nabla f(\boldsymbol{\theta}^t)\|^2 \\
&\quad + \left(\frac{\eta_l L^2}{2n} + \frac{L\eta_l^2\tau^2(\phi_k+1)L^2}{n\tau}\right)\sum_{i=1}^n\sum_{s=0}^{\tau-1}\mathbb{E}_t\|\boldsymbol{\theta}^t - \boldsymbol{\theta}_{i,s}^{t,s}\|^2 + \frac{\eta_l\tau\phi_k\bar{\zeta}^2}{2\gamma} \\
&\quad + L\eta_l^2\tau^2(\phi_k+1)(2\kappa^2 + \bar{\zeta}^2) + \frac{LkC^2\sigma^2}{2r^2} \\
&\leq -\frac{\eta_l\tau}{4}\|\nabla f(\boldsymbol{\theta}^t)\|^2 + \frac{\eta_l L^2(4\beta^2+1)}{8n\beta^2}\sum_{i=1}^n\sum_{s=0}^{\tau-1}\mathbb{E}_t\|\boldsymbol{\theta}^t - \boldsymbol{\theta}_{i,s}^{t,s}\|^2 + \frac{\eta_l\tau\phi_k\bar{\zeta}^2}{2\gamma} \\
&\quad + L\eta_l^2\tau^2(\phi_k+1)(2\kappa^2 + \bar{\zeta}^2) + \frac{LkC^2\sigma^2}{2r^2} \tag{42}
\end{aligned}$$

if $\eta_l \leq (1-2\gamma)/8\tau L(\phi_k+1)\beta^2$ and $\gamma < 1/2$. Then, by Lemma 10, we have

$$\begin{aligned}
\mathbb{E}_t[f(\boldsymbol{\theta}^{t+1}) - f(\boldsymbol{\theta}^t)] &\leq -\frac{\eta_l\tau}{4}\|\nabla f(\boldsymbol{\theta}^t)\|^2 + \frac{\eta_l L^2(4\beta^2+1)}{8\beta^2}\sum_{s=0}^{\tau-1}\left[32\eta_l^2\tau^2\beta^2\|\nabla f(\boldsymbol{\theta}^t)\|^2 + 32\eta_l^2\tau^2\kappa^2 + 4\tau\eta_l^2\bar{\zeta}^2\right] + \frac{\eta_l\tau\phi_k\bar{\zeta}^2}{2\gamma} \\
&\quad + L\eta_l^2\tau^2(\phi_k+1)(2\kappa^2 + \bar{\zeta}^2) + \frac{LkC^2\sigma^2}{2r^2} \\
&\leq \left(-\frac{\eta_l\tau}{4} + 4\eta_l^3\tau^3L^2(4\beta^2+1)\right)\|\nabla f(\boldsymbol{\theta}^t)\|^2 + \frac{\eta_l^3\tau^2L^2(4\beta^2+1)(8\tau\kappa^2 + \bar{\zeta}^2)}{2\beta^2} + \frac{\eta_l\tau\phi_k\bar{\zeta}^2}{2\gamma} \\
&\quad + L\eta_l^2\tau^2(\phi_k+1)(2\kappa^2 + \bar{\zeta}^2) + \frac{LkC^2\sigma^2}{2r^2} \\
&\leq -\frac{\eta_l\tau}{8}\|\nabla f(\boldsymbol{\theta}^t)\|^2 + \eta_l^2\tau^2L(24\eta_l\tau L + 2)\kappa^2 + \eta_l^2\tau^2L(3\eta_l L + 1)\bar{\zeta}^2 \\
&\quad + \left(L\eta_l^2\tau^2(2\kappa^2 + \bar{\zeta}^2) + \frac{\eta_l\tau\bar{\zeta}^2}{2\gamma}\right)\phi_k + \frac{LkC^2\sigma^2}{2r^2} \\
&\leq -\frac{\eta_l\tau}{8}\|\nabla f(\boldsymbol{\theta}^t)\|^2 + \eta_l^2\tau^2L(3\kappa^2 + 2\bar{\zeta}^2) + \left(L\eta_l^2\tau^2(2\kappa^2 + \bar{\zeta}^2) + \frac{\eta_l\tau\bar{\zeta}^2}{2\gamma}\right)\phi_k + \frac{LkC^2\sigma^2}{2r^2}, \tag{43}
\end{aligned}$$

if $\eta_l \leq \min\{1/4\tau L\sqrt{8\beta^2 + 2}, 1/24\tau L\}$. Rearranging the above inequality in (43) and summing it from $t = 0$ to $T - 1$, we get

$$\sum_{t=0}^{T-1} \|\nabla f(\boldsymbol{\theta}^t)\|^2 \leq \frac{8}{\eta_l \tau} \sum_{t=0}^{T-1} \mathbb{E}_t[f(\boldsymbol{\theta}^{t+1}) - f(\boldsymbol{\theta}^t)] + 8T\eta_l \tau L(3\kappa^2 + 2\bar{\zeta}^2) + 8T \left(\eta_l \tau L(2\kappa^2 + \bar{\zeta}^2) + \frac{\bar{\zeta}^2}{2\gamma} \right) \phi_k + \frac{4TLkC^2\sigma^2}{\eta_l \tau r^2}, \quad (44)$$

where the expectation is taken over all rounds $t \in [0, T - 1]$. Dividing both sides of (44) by T , one yields

$$\frac{1}{T} \sum_{t=0}^{T-1} \|\nabla f(\boldsymbol{\theta}^t)\|^2 \leq \frac{8(f(\boldsymbol{\theta}^0) - f^*)}{T\eta_l \tau} + 8\eta_l \tau L(3\kappa^2 + 2\bar{\zeta}^2) + 8 \left(\eta_l \tau L(2\kappa^2 + \bar{\zeta}^2) + \frac{\bar{\zeta}^2}{2\gamma} \right) \phi_k + \frac{4LkC^2\sigma^2}{\eta_l \tau r^2},$$

Here, we use the fact that $f^* \leq f(\boldsymbol{\theta}^T)$. Theorem 2 follows by summarizing the convergence results of Fed-SMP with rand_k sparsifier and top_k sparsifier and letting $\gamma = 1/3$.